

AEROSPACE EXAMPLE

Descriptions

Figure 1 shows a schematic of a one degree-of-freedom control system for the rudder of an aircraft wing. The adjustment of the wing is shown by a single-rod hydraulic actuator which moves in a linear direction to adjust the angle of the rudder shown by the symbol d . The moment arm of the linkage is shown by the symbol L and the displacement of the actuator is shown by the dimension y . The hinge moment acting on the rudder is shown by the symbol H and as discussed later, this moment is proportional to the rudder angle d .

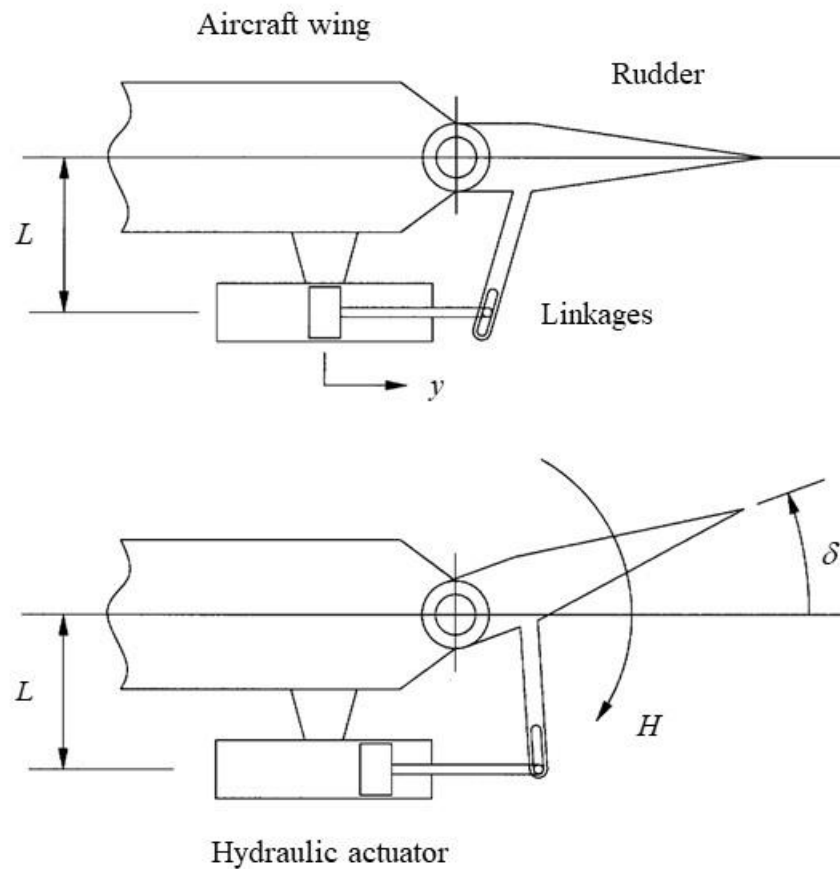


Figure 1. Schematic of the control rudder for the flight control surface of an aircraft wing

Kinematic Analysis

The kinematic analysis for the aircraft-wing linkage shown in Fig. 1 is quite simple as the geometry of a right triangle shows:

$$\tan(d) = \frac{y}{L} . \quad (1)$$

For small values of d a Maclaurin series may be used to show that

$$d = \frac{y}{L} . \quad (2)$$

This result is quite important and illustrates that the rudder angle for the flight control surface is proportional to the linear displacement of the hydraulic actuator.

Kinetic Analysis

From a quasi-steady analysis of moments acting on the flight control surface, shown in Fig. 1, it may be shown that the actuator force required for resisting the hinge moment H is given by

$$F = \frac{H}{L} , \quad (3)$$

where the hinge moment is given by

$$H = \bar{q}_\infty S_r c_r C_H d . \quad (4)$$

In this equation, \bar{q}_∞ is the dynamic pressure of the air passing over the rudder, S_r is the rudder area, c_r is the rudder mean cord, C_H is the hinge moment coefficient, and d is the rudder angle shown in Fig. 1. Typical values for a single flight control surface are given in the following table:

Description	Symbol	Quantity	Units
Dynamic pressure	\bar{q}_\forall	300	lbf/ft ²
Rudder area	S_r	5	ft ²
Rudder mean cord	c_r	1.5	ft
Hinge moment coefficient	C_H	1.6	no units

Hydraulic System Modeling

Actuator Description. The hydraulic actuator shown for the flight control surface in Fig. 1 is controlled using a hydraulic power supply and a 3-way control valve for porting fluid in and out of the actuator. A detailed schematic for the actuator is shown Fig. 2 where the controlled displacement of the actuator to the right is shown by the symbol y . The force acting on the actuator is shown by the symbol F and the fluid pressures on sides A and B of the actuator are given by the symbols P_A and P_B respectively. Since side- B is directly connected to the discharge pressure of the pump $P_B = P_p$. The pressurized areas on both sides of the actuator are given by A_A and A_B .

The 3-way valve shown in Fig. 2 moves back and forth in the x -direction in order to port fluid in and out of side A of the actuator. The volumetric flow rate into side A is shown using the symbol Q_A while the volumetric flow rate out of side B is shown by the symbol Q_B . The valve is designed as an open-centered valve which means that the metering lands are open when the valve is in the null position $x = 0$. The nominal opening for each metering land is shown in Fig. 2 by the symbol u which is often called an underlapped dimension.

The hydraulic power supply to the open-centered 3-way valve is shown in Fig. 2 by a pressure compensated, variable displacement pump. This pump is automatically controlled to provide enough flow Q_p in order to maintain the supply pressure P_p . The torque and rotational speed of the pump shaft are shown by the symbols T and ω .

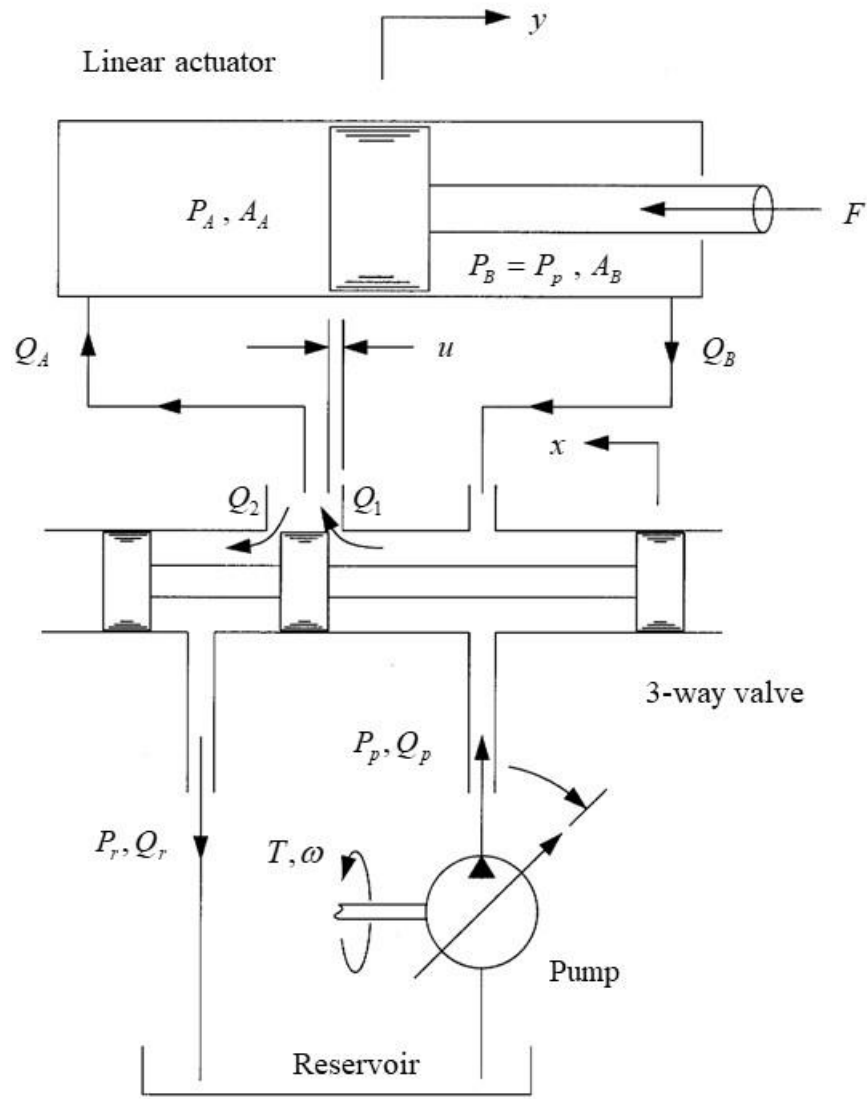


Figure 2. Schematic for hydraulic, linear actuator

The pump reservoir is shown to have a pressure P_r which will be assumed to be atmospheric pressure in the analysis which follows. The volumetric flow rate returned to the reservoir by the 3-way valve is shown in Fig. 4 by the symbol Q_r .

Quasi-Steady Analysis. By neglecting the time rate-of-change of linear momentum for the actuator and its load, the following quasi-steady equation may be written to describe the load force acting on the actuator:

$$F = P_A A_A - P_p A_B \quad . \quad (5)$$

By neglecting the pressure transients on sides A and B of the actuator, the volumetric flow rate into the actuator on side A and out of the actuator on side B may be written as

$$Q_A = A_A \dot{y} \quad (6)$$

where the dot notation over the symbol y is used to denote a time derivative. Equations (5) and (6) will provide the basic model for resisting and moving the actuator load.

Volumetric Flow Rate. As shown in Eq. (6) the volumetric flow rate in and out of the actuator is what moves the actuator to the right or left. For an incompressible fluid, the conservation of mass requires that

$$Q_A = Q_1 - Q_2 \quad (7)$$

where each flow rate is shown schematically in Fig. 2. If we assume that the port area for each metering land on the 3-way valve opens linearly with respect to the valve displacement x , then using the classical orifice equation the volumetric flow rate across each metering land may be written as

$$Q_1 = h(u+x)C_d \sqrt{\frac{2}{r}(P_p - P_A)} \quad , \quad Q_2 = h(u-x)C_d \sqrt{\frac{2}{r}(P_A - P_r)} \quad . \quad (8)$$

In this result h is the area gradient of the valve port, u is the underlapped dimension as previously noted, C_d is the dimensionless discharge coefficient, ρ is the fluid density, and all other variables have been previously defined. Substituting Eq. (8) into Eq. (7) and linearizing the result about nominal operating conditions produces the following linearized results for the volumetric flow rate in and out of the actuator:

$$Q_A = K_q(x - x_o) - K_c(P_A - P_{A_o}) \quad , \quad (9)$$

where the subscript “o” denotes a nominal condition and the flow gain and pressure-flow coefficient are given by

$$K_q = h C_d \sqrt{\frac{2}{\rho} P_p} \left(\sqrt{1 - \frac{P_{A_o}}{P_p}} + \sqrt{\frac{P_{A_o}}{P_p}} \right) \quad , \quad K_c = \frac{u h C_d}{\sqrt{2 \rho P_p}} \left(\frac{1 + \frac{x_o}{u}}{\sqrt{1 - \frac{P_{A_o}}{P_p}}} + \frac{1 - \frac{x_o}{u}}{\sqrt{\frac{P_{A_o}}{P_p}}} \right) \quad . \quad (10)$$

Nominal Operating Condition. In order to evaluate the nominal operating conditions of the system we recognize at steady-state conditions (no motion) $Q_A = 0$, which means that $Q_1 - Q_2 = 0$. Using these relationships with Eq. (8) it may be shown that the following nominal-relationship must exist at steady-state conditions:

$$\left(\frac{u + x_o}{u - x_o} \right)^2 = \frac{P_{A_o}}{P_p - P_{A_o}} \quad . \quad (11)$$

Using this result with a steady-state form of Eq. (5), the following nominal operating condition may be determined:

$$P_{A_o} = \frac{A_B P_p + F_o}{A_A} \quad \text{and} \quad x_o = \frac{C - 1}{C + 1} u \quad , \quad (12)$$

where F_o is the nominal force acting on the actuator and

$$C = \sqrt{\frac{A_B P_p + F_o}{(A_A - A_B) P_p - F_o}} \quad (13)$$

These results may be used to model the hydraulic actuator as a linear system near the nominal operating points.

If we assume that the nominal operating conditions are determined when the rudder angle $\delta = 0$, Eq. (4) may be used to show that $F_o = 0$. Using these conditions with the previous analysis, it may also be shown that

$$P_{A_o} = \frac{1}{2} P_p \quad \text{and} \quad x_o = 0 \quad (14)$$

as long as the following design condition is enforced:

$$A_B = \frac{1}{2} A_A \quad (15)$$

It may also be shown that the flow gain and the pressure flow coefficient reduce to the following form:

$$K_q = 2 h C_d \sqrt{\frac{P_p}{r}} \quad , \quad K_c = \frac{2 u h C_d}{\sqrt{r P_p}} \quad (16)$$

Summary. Using the preceding analysis with Eqs. (5) and (6), the velocity of the rudder angle and the fluid pressure on side A may be solved for algebraically as

$$\dot{\delta} = \frac{K_q}{A_A L} x - \frac{K_c}{A_A L} \left(\frac{\bar{q}_\infty S_r c_r C_H}{A_A L} \right) \delta \quad \text{and} \quad P_A = \left(\frac{\bar{q}_\infty S_r c_r C_H}{A_A L} \right) \delta + \frac{1}{2} P_p \quad (17)$$

In the subsequent sections, these equations will be used to demonstrate position control for the flight control surface shown in Fig. 1.

Model Analysis and Hydraulic System Design

Model analysis. Let the input to the model be a step input of magnitude x_{ref} ,

$$x(t) = \begin{cases} 0 & \text{if } t \leq 0 \\ x_{ref} & \text{if } t > 0 \end{cases} \quad (18)$$

The solution of the differential equation in Eq. (17) with input given by Eq. (18) can be found to be the following:

$$d(t) = (1 - e^{-t/t}) M x_{ref},$$

where

$$t = \frac{(A_A L)^2}{K_c \bar{q}_v S_r c_r C_H} \quad \text{and} \quad M = \frac{K_q A_A L}{K_c \bar{q}_v S_r c_r C_H}.$$

In this equation, M is the steady state relationship between the input and the output, known as the DC gain, and t is the inverse of the exponential decay rate, known as the time constant. These two parameters can be used to characterize the time response of first-order systems and are often used to describe the performance of these systems.

Hydraulic system design. For the design of the hydraulic and mechanical system, we will set the following parameters listed in the table below.

Description	Symbol	Quantity	Units
Rudder angle maximum	d_{max}	45	°
Moment arm length	L	8	inch
Hydraulic fluid density	r	53	lbm / ft ³
Pump supply pressure	P_p	2500	psi
Orifice discharge coefficient	C_d	0.62	no units

Several other parameters must be designed to fit the rudder control application. The required cylinder length to achieve the maximum angle of the rudder is,

$$L_c = 2 \tan(d_{max}) L = 1.33 \text{ ft.}$$

If we choose the maximum time needed to move the rudder through

its full range of travel to be 3 seconds, then the required maximum velocity of

$v_o = L_C / 3 \text{ seconds} = 0.44 \text{ ft / second}$. If we evaluate H at the maximum rudder angle, then we

get $H_{\max} = 2,827 \text{ lbf-ft}$. Then we can compute the maximum force, $F_{\max} = H_{\max} / L = 4,241 \text{ lbf}$.

Finally, we can design the cylinder size to produce the maximum required force at $1/2$ of the

supply pressure as follows: $A_A = F_{\max} / (P_p / 2) = 3.393 \text{ inch}^2$. The valve may be designed to

have an underlap dimension, u , of,

$$u = \sqrt{\frac{A_A v_o}{2C_d \sqrt{P_p / r}}} = 0.0042 \text{ inch}, \quad (20)$$

and a circumference of $h = 4u = 0.2040 \text{ inch}$ [1].

Position Control

Control structure. A position control system is needed to control the rudder using the measurement of the output d and a desired rudder position d_d to determine the control effort (valve position x) to produce responses with error, e , that is low and reduced to a low value quickly. We can define the error as

$$e(t) = d_d - d(t). \quad (21)$$

In order to reduce the error, a simple control system can be implemented using error in the following equation,

$$x(t) = K(d_d - d(t)), \quad (22)$$

where K is a control gain. During operation of the controller, the error will be multiplied by K , if the measured rudder angle is smaller than desired, the error is positive, so the control effort, x ,

will be positive, shifting the valve to send more flow to the hydraulic cylinder to move the rudder in the positive direction. The opposite is true if the measured rudder angle is too large.

Design requirements. Let's choose design requirements so that the steady state error is 10% of a step change in the desired position and the speed of response is quantified by a settling time of 0.040 seconds after a step change in the desired rudder position given in Eq. (23).

$$\begin{aligned} \text{Steady state error: } e_{ss} &= 0.10 \text{ (10\%)} \\ \text{Settling time: } t_s &= 0.040 \text{ sec.} \end{aligned} \tag{24}$$

To design the control system, a value of K must be found to satisfy the design requirements in Eq. (24).

The design requirements can now be applied to the dynamic system equations of the model in Eq. (17) and the simple control system of Eq. (22). By combining these equations, the closed-loop controlled system response can be found as,

$$\begin{aligned} d(t) &= (1 - e^{-t/t_{cl}}) M_{cl} d_d, \\ \text{where} & \\ t_{cl} &= \left(\frac{1}{t} - \frac{K_q K}{A_A L} \right)^{-1} \quad \text{and} \quad M_{cl} = MK t_{cl}. \end{aligned} \tag{25}$$

Equation (25) tells us that increasing K to a large value will cause the closed-loop time constant, t_{cl} , to become small, indicating a time response that is faster. Given a desired, closed-loop time constant, a control gain can be found by solving the closed loop time constant for K ,

$$K = \left(\frac{1}{t_{cl}} - \frac{1}{t} \right) \frac{A_A L}{K_q}. \tag{26}$$

This equation allows the control system to achieve any desired closed-loop time constant which gives the designer the ability to arbitrarily choose the desired time response of the system.

Another important design goal is steady state error, which is the steady value of Eq. (21).

To find the steady error, first substitute the result in Eq. (25) into Eq.(21) and take the limit as time approaches infinity to get,

$$e_{ss} = \left[1 - \frac{K_q A_A LK}{\left(K_c \bar{q}_\infty S_r c_r C_H + K_q A_A LK \right)} \right] d_d. \quad (27)$$

This equation tells us that if K is chosen as large as is possible, the steady state error will be as small as possible but not ever zero. Therefore, choosing a large value of K achieves both goals of a fast time response and a small steady state error. The maximum feasible value of the valve displacement is at least one practical limitation associated with choosing a large value of K . As can be seen from Eq. (22), increasing the value of K causes the value of x to become large when there is large error between the desired and actual value of the rudder position.

Results and Discussion

Analytical results. The following numerical results demonstrate the use of the equations above for analyzing the system and designing a controller. Calculated using Eq. (19), the time constant of the system without a controller is somewhat slow at $t = 0.5890$ sec. If a settling time of 16 ms is desired for the closed-loop control system, then a value of one fourth of the settling time can be used to find the design requirement for the closed-loop time constant [2],

$t_{CL} = 0.040$ sec. The design requirement for the closed-loop time constant can be used in Eq.

(26) to compute the required control gain, $K = 0.0078$ inch/deg. Using Eq. (27), the steady state error given a step input is 6.8% of the value of the desired angle, which is less than the stated design requirement. If a smaller error level is desired a larger value of K could be selected which would also increase the speed of the time response of the control system.

Simulations. To demonstrate the control design, a simulation has been created (Figures 3-5) by evaluating the differential equations that describe the system. Equation (25) has been evaluated with a 5-degree step input supplied for the desired rudder angle (Figure 3). This simulation shows that the rudder angle settled to within 98% of its final value within 16 ms but did not reach the desired position. Figure 3 also demonstrates an important characteristic of first order dynamic systems; there is no overshoot in the response. In Figure 4, the error, Eq. (21), is plotted showing that the error started at 5 degrees and reduced to a low value over time, approaching 6.8% of the desired rudder angle. To reduce the error, a larger control gain could be selected or a different type of controller could be selected that could apply more control effort to reduce the error further. As stated before, another important aspect of the control system is control effort in Eq. (22) which is plotted in Figure 5. This plot shows that the control effort (valve position) is relatively low at its steady state position, suggesting that more control effort is possible to reduce the steady error. The plot of the control effort could also be used to determine if the valve position would have a displacement beyond the physical limits of the valve design, which could suggest the need for a redesign of the controller or the physical valve components.

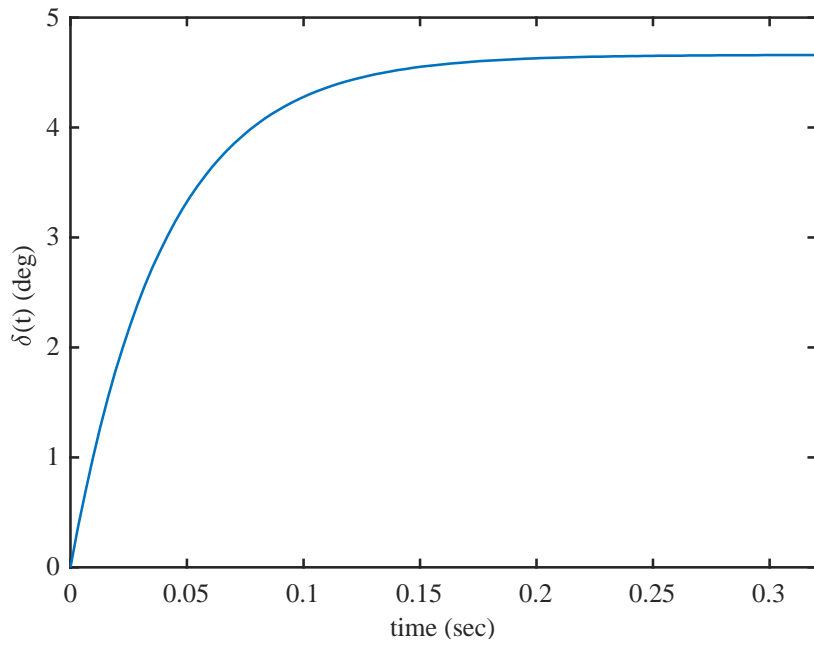


Figure 2. Closed-loop control system response due to a 5-degree step input supplied to the desired rudder angle.

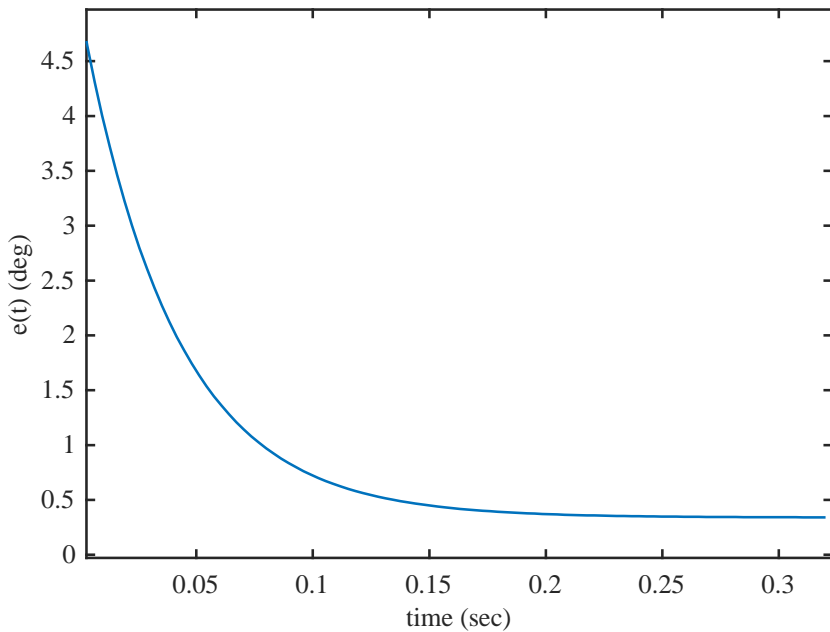


Figure 4. Closed-loop response of error due to a 5-degree step input supplied to the desired rudder angle.

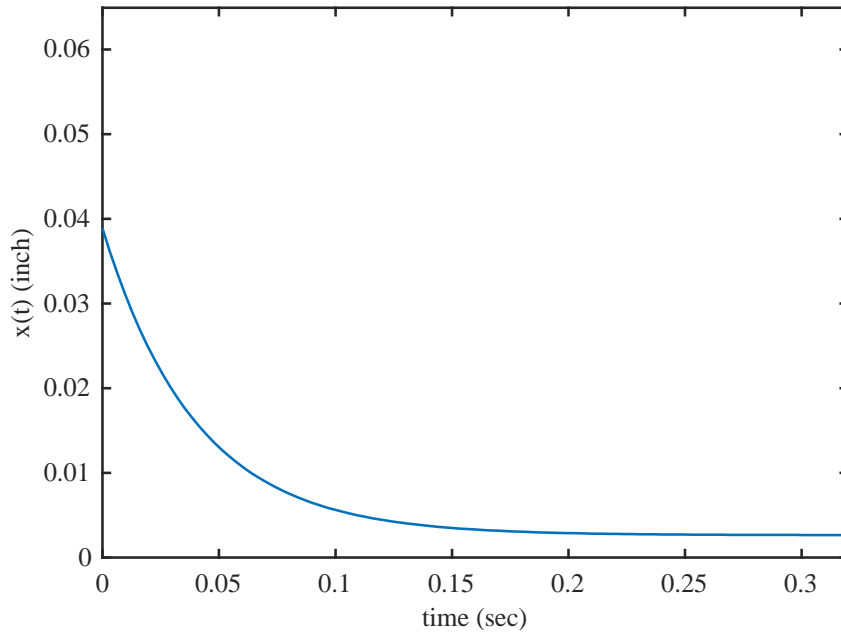


Figure 5. Closed-loop response of control effort (valve position) due to a 5-degree step input supplied to the desired rudder angle.

Conclusions

After some simplifications, the dynamics of the aircraft rudder and the hydraulic system that includes a 3-way valve-controlled linear actuator can be modeled by a linear first order ordinary differential equation. Using some basic design principles starting with the load on the rudder, the parameters of the model can be found for the given aircraft application. A simple control system with a single control gain can be used to achieve rudder position control requirements, low steady state error and a fast response to a step change in the desired rudder angle. Both analysis and simulations verify the control design results. A re-design of the control system could be pursued to increase the speed of response and the steady state error by

increasing the gain if desired. Any design or re-design of the controller should include a check of the control effort to make sure that the value of the valve displacement is not too high.

References

[1] Manring, Noah D. 2005. *Hydraulic control systems*. John Wiley & Sons, Hoboken, NJ.

[2] Kluever, C.A., 2015. *Dynamic systems: modeling, simulation, and control*. John Wiley & Sons, Hoboken, NJ.

TRACK-TYPE TRACTOR EXAMPLE

Descriptions

Figure 1 shows a schematic of a track-type tractor that uses a hydrostatic differential-steering system in conjunction with a mechanical transmission to alter the angular direction of the vehicle. As shown in this figure, the vehicle has a symmetrical right and left track. The amount of track engaged with the ground is shown by the symbol L and the width of each track is shown by the symbol w . The outside radius of curvature for the track is shown by the symbol R . The track base for the tractor is shown by the quantity $2d$. The vehicle has a total mass given by M and the mass moment-of-inertia for the vehicle at the mass center, and about an axis out of the paper, is given by the symbol J .

As the vehicle moves forward in the x -direction, it is propelled by tractive forces acting on the right and left track shown in Fig. 1 by the symbols F_R and F_L respectively. These forces are designed to overcome either a pushing or pulling force shown in the figure by the symbol P . When the vehicle turns, the forward direction of the right track, x_R , become different than the forward direction of the left track, x_L , producing an angular orientation for the vehicle shown by the symbol Θ . This angular orientation describes the steering direction for the vehicle which is altered by the control of a hydrostatic transmission working in conjunction with a mechanical transmission on both the right and left sides of the vehicle. Each track of the vehicle is driven by a planetary gear that receives power through a mechanical path and hydrostatic path (for steering). All vehicle power is provided by the engine.

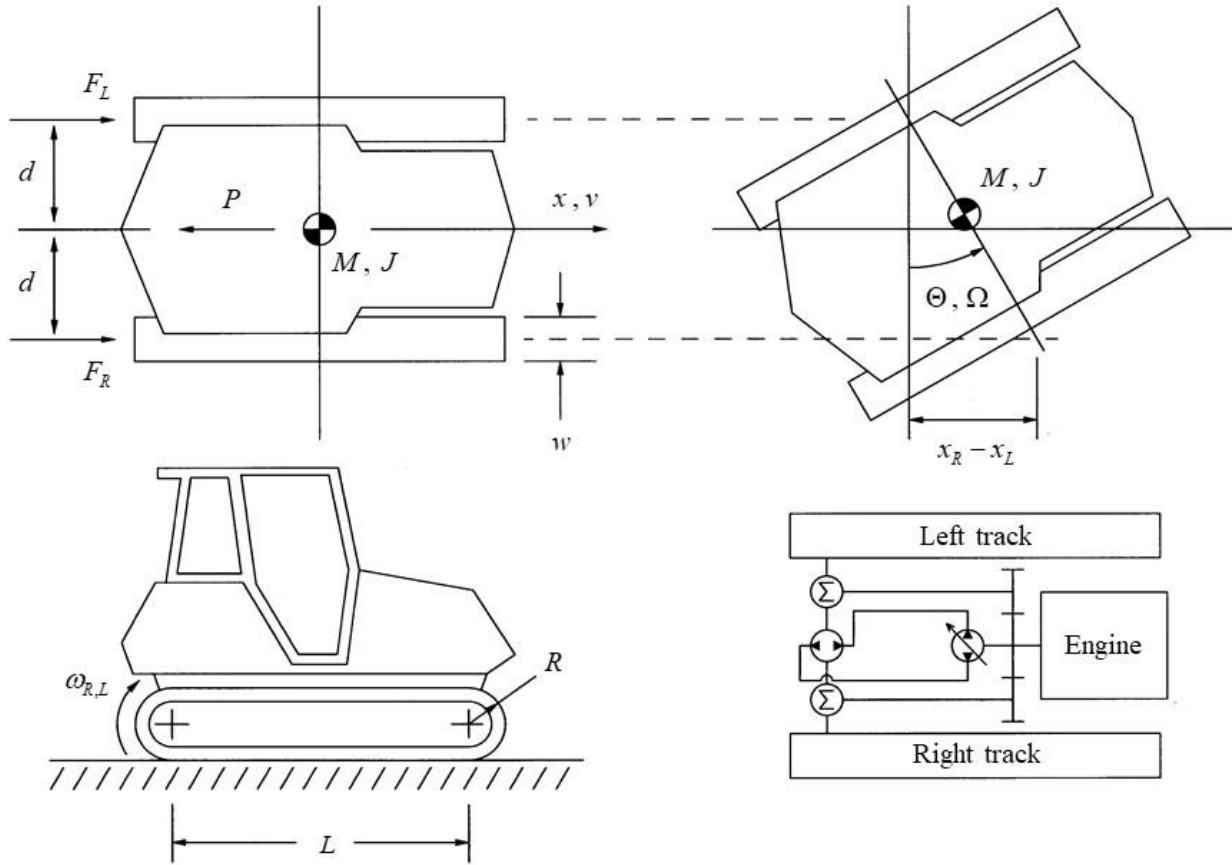


Figure 1. Schematic of track-type tractor with a differential-steering system

Vehicle Model

Equations of Motion. The equations of motion for the track-type tractor shown in Fig. 1 are determined using Newton's second law for the time rate-of-change of linear and angular momentum for the vehicle. These equations are presented as

$$M\ddot{x} = F_R + F_L - P \quad \text{and} \quad J\ddot{\Theta} = d(F_R - F_L) \quad . \quad (1)$$

All of the symbols in this equation are shown in Fig. 1 and have been previously described. The following kinematic relationship will be useful as the analysis below unfolds:

$$x = \frac{x_R + x_L}{2} \quad \text{and} \quad \Omega = \frac{x_R - x_L}{2d} \quad (2)$$

The first relationship simply says that the forward displacement of the tractor is equal to the average displacement of each track. The second relationship is a linearized form of the angular displacement of the tractor that results when the right and left tracks undergo a difference in displacement.

Tractive Effort. The tractive effort for a single track of the vehicle has been derived in previous work [1] and is presented here as follows:

$$F = A \frac{W}{2} \left[1 - \frac{K}{sL} \left(1 - \text{Exp} \left\{ \frac{-sL}{K} \right\} \right) \right], \quad \text{where} \quad A = \frac{2wcL}{W} + \tan(g) \quad . \quad (3)$$

In this equation, W is the total weight of the vehicle, L and w are track dimensions shown in Fig. 1, K is the shear deformation modulus of the terrain, g is the shear angle of the soil, c is the cohesion constant of the soil, and s is a nondimensional description of the slippage of the track with respect to the soil that may vary between zero and unity (to be discussed later). A important thing to notice from the traction model presented in Eq. (3) is that tractive effort depends upon some amount of slippage between the track and the terrain. In other words, the slippage coefficient s must always be greater than zero if tractive effort is to be generated. Since track-type tractors are designed to operate on loose terrain, this requirement for our model is not unrealistic.

If we linearize Eq. (3) about the nominal operating conditions of the tractor, the following result may be written:

$$F = \frac{P_o}{2} + B \frac{P_o (s - s_o)}{2 (1 - s_o)} \quad , \quad \text{where} \quad B = \frac{L}{K} \left(A \frac{W}{P_o} - \frac{K}{Ls_o} - 1 \right) (1 - s_o) \quad . \quad (4)$$

In this equation P_o is the nominal load being pushed or pulled by the tractor, and s_o is the nominal slippage coefficient for the track to be discussed in the next paragraph.

Track Slippage. As previously mentioned, track slippage is required to achieve tractive effort between the tractor and the ground. For a single track, this slippage is defined as

$$s = 1 - \frac{\dot{x}}{R \omega} \quad (5)$$

where \dot{x} is the absolute velocity of the track in the forward direction, R is the radius of curvature for the track shown in Fig. 1, and ω is the angular velocity of the track about the axis shown in Fig. 1. From this result it may be seen that when $s = 1$ the vehicle is not moving and the track is in pure slip. When $s = 0$ there is no slippage between the track and the ground. As previously mentioned this condition cannot exist if tractive effort is desired.

A linearized form of Eq. (5) may be obtained as follows:

$$(s - s_o) = (1 - s_o) \left[\frac{\omega}{\omega_o} - \frac{\dot{x}}{v_o} \right] , \quad (6)$$

where ω_o is the nominal angular velocity for the track and v_o is the nominal absolute velocity for the track in the forward direction. This result will be used in the next paragraph to summarize the linearized equations of motion for the track-type tractor.

Summary. By combining the preceding results, the time rate-of-change of linear momentum for the track-type tractor may be expressed as

$$M \dot{v} + \left(\frac{BP_o}{v_o} \right) v = \left(\frac{BP_o}{2\omega_o} \right) (\omega_R + \omega_L) - (P - P_o) . \quad (7)$$

Similarly, the time rate-of-change of angular momentum for the vehicle is given by

$$J \dot{\Omega} + \left(\frac{d^2 BP_o}{v_o} \right) \Omega = \left(\frac{d BP_o}{2\omega_o} \right) (\omega_R - \omega_L) . \quad (8)$$

In these equations, v and Ω are the translational velocity and the angular velocity of the tractor respectively as shown in Fig. 1. The inputs are the angular velocities of the right and left tracks,

Governing Equations. As previously noted, the carrier of each planetary gear set is used to convey power to the tracks. The drive wheel of each track is connected to the carrier through a final-drive gear box, which has a speed ratio given by m_{FD} (not shown in any figure). For a single track, the following equations may be written to describe the relationship between the carrier angular-velocity and torque, and the track angular-velocity and torque:

$$W_c = m_{FD} W \quad \text{and} \quad m_{FD} T_c = F R \quad (9)$$

where F is the tractive effort on the track described in Eq. (4), and R is the track radius of curvature shown in Fig. 1.

The equations which govern the kinematics and the kinetics of each planetary gear set are presented without derivation as follows:

$$m_r W_r + W_s - m_c W_c = 0 \quad , \quad T_c + m_c T_s = 0 \quad , \quad T_r - m_r T_s = 0 \quad (10)$$

where the speed ratio for the ring and the carrier are given respectively as

$$m_r = \frac{r_r}{r_s} \quad \text{and} \quad m_c = \frac{2r_c}{r_s} \quad . \quad (11)$$

The hydraulic motor is used for steering the tractor, and is depicted in Fig. 2 as a single gear with a pitch radius given by r_m . The equations which describe the kinematics and kinetics of this gear are given by:

$$W_m - m_m W_{r_R} = 0 \quad , \quad W_m + m_m W_{r_L} = 0 \quad , \quad m_m T_m + T_{r_R} - T_{r_L} = 0 \quad (12)$$

where the speed ratio for the hydraulic motor is given by

$$m_m = \frac{R}{r_m} \quad . \quad (13)$$

The engine for the tractor supplies power to the tracks through the sun gear of each planetary gear set. For the purposes of this analysis, we simply need the following relationship

for the kinematics of this power transmission:

$$W_{s_R} = W_{s_L} = m_e W_e \quad (14)$$

where m_e is the speed ratio between the engine and the sun gear, and W_e is the angular velocity for the engine.

Summary. The previous equations may be combined to produce the following kinematic results for angular velocity of the right and left track:

$$W_R = X_m W_m + X_e W_e \quad \text{and} \quad W_L = -X_m W_m + X_e W_e \quad (15)$$

where the overall speed ratios for the hydraulic motor and the engine are given by

$$X_m = \frac{m_r}{m_{FD} m_c m_m} \quad \text{and} \quad X_e = \frac{m_e}{m_{FD} m_c} \quad (16)$$

Another useful result from this analysis is the torque that is generated on the hydraulic motor during tractor operation. This torque is given by

$$T_m = X_m (F_R - F_L) R \quad (17)$$

where X_m is given in Eq. (16).

Hydraulic System Modeling

Figure 3 shows a schematic for the hydraulic transmission that is used to control the steering of the track-type tractor. As shown in this figure, the transmission is comprised of a fixed displacement motor and a variable displacement pump. The angular velocity of the pump (which is generally the angular velocity of the engine) is shown by the symbol W_p while the angular velocity of the motor is again shown by the symbol W_m . The volumetric displacement for the pump and motor are given by the symbols V_p and V_m respectively. The instantaneous

displacement of the pump is controlled by the swash plate angle which is illustrated in Fig. 3 by the symbol $\hat{\alpha}$ which can vary between -1 and +1. The pressure in the hydraulic transmission line is shown by the symbol p while the volumetric flow rate across the motor is given by Q .

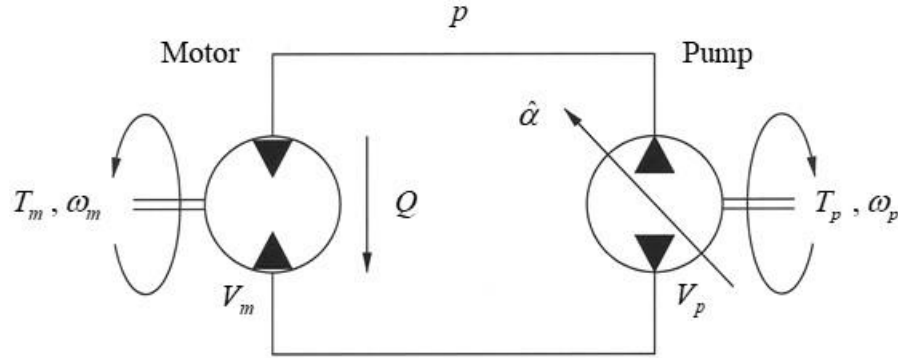


Figure 3. Hydraulic transmission used for controlling the steering of the track-type tractor

If we neglect the internal leakage of the transmission, it may be shown by equating the volumetric flow rate of the pump with the volumetric flow rate of the motor, that the angular speed of the transmission is given by

$$\omega_m = \frac{V_p}{V_m} \omega_p \hat{\alpha} \quad . \quad (18)$$

Furthermore, the fluid pressure in the transmission line may be calculated using the following equation:

$$p = \frac{T_m}{V_m} \quad (19)$$

Where the torque on the motor is shown in Eq. (17). Using the previous analysis it may be shown that this fluid pressure is given more explicitly by

$$p = \frac{BP_o X_m R}{V_m} \left(\frac{X_m W_p V_p}{W_o V_m} \hat{\alpha} - \frac{d}{v_o} W \right) . \quad (20)$$

This equation is important for sizing the transmission and avoiding an over-pressurized transmission line.

Equation Summary

By combining the previous analysis the following equations of motion for the track-type tractor may be written:

$$M \dot{v} + \left(\frac{BP_o}{v_o} \right) v = \left(\frac{BP_o \xi_e}{\omega_o} \right) \omega_e - (P - P_o) , \quad (21)$$

and

$$J \dot{\Omega} + \left(\frac{d^2 BP_o}{v_o} \right) \Omega = \left(d BP_o \xi_m \frac{V_p}{V_m} \frac{\omega_p}{\omega_o} \right) \hat{\alpha} . \quad (22)$$

The inputs to these equations are engine speed ω_e for translational velocity, and swash plate angle $\hat{\alpha}$ for steering.

A typical set of physical values for a system like this are given in the following table:

Description	Symbol	Value	Units
Nominal load	P_o	118,211	N
Nominal slip	s_o	0.10	No units
Nominal angular track velocity	W_o	49.80	rpm
Nominal engine speed	W_e	2,000	rpm
Vehicle mass	M	24,100	kg
Vehicle mass moment-of-inertia	J	40,616	kg m ²

Description	Symbol	Value	Units
Vehicle weight	W	236,421	N
Half track base	d	1.130	m
Track radius	R	0.381	m
Track length	L	3.888	m
Track width	w	0.610	m
Soil cohesion constant	c	3,100	Pa
Soil shear angle	g	0.520	rad
Soil deformation modulus	K	0.025	m
Calculated tractive effort constant	A	0.635	No units
Calculated tractive effort constant	B	28.706	No units
Engine speed ratio	$1 / \chi_e$	40.16	No units
Hydraulic motor speed ratio	$1 / \chi_m$	240.98	No units
Pump speed	W_p	2,000	rpm
Pump displacement	V_p	140	cc/rev
Motor displacement	V_m	140	cc/rev

Analysis of the Model

The two differential equations for the model are first-order and are independent. However, if we consider the angular orientation rather than the rate of change of the angular orientation, Eq. (22) becomes a second order equation. The differential equation for the orientation angle dynamics, using Eq. (22), can be written as follows:

$$\ddot{\Theta}(t) + a \dot{\Theta}(t) = b \hat{\alpha}(t),$$

where,

$$a = \frac{d^2 B P_o}{J v_o}, \text{ and } b = d B P_o \xi_m \frac{V_p}{V_m} \frac{\omega_p}{\omega_o} \frac{1}{J}. \quad (23)$$

The solution to this differential equation given a step input of magnitude a_{ref} ,

$$\hat{\alpha}(t) = \begin{cases} 0 & \text{if } t \leq 0 \\ a_{ref} & \text{if } t > 0 \end{cases} \quad (24)$$

can be found as,

$$Q(t) = \frac{a_{ref} b}{a} \left[t + \frac{1}{a} (1 - e^{-at}) \right] \quad (25)$$

This solution has a few characteristics of interest. The solution does not exponentially increase to infinity as time increases, so the system is not unstable. However, the solution does not decay to zero, although one of the terms in the equation does have a negative exponential decay which will decay to zero as time approaches infinity. One of the terms of the solution includes the time, t , which will linearly increase as time increases. This characteristic is undesirable in the absence of a feedback controller to adjust the input. However, when feedback is applied, this linearly increasing characteristic of the orientation angle will act in a way that actually makes controlling steady-state error an easier task.

Position Control

Performance requirements. Several different control objectives may be considered in the track-type tractor steering system. These include tracking of a desired path, desired speed, desired rate of change in the orientation angle, and desired orientation angle. In a typical automatic guidance system, the vehicle is pointed toward a goal location while the speed is separately controlled. This is similar to a vehicle operator picking a goal destination in the

distance and steering the vehicle toward that goal. To follow a path the goal location is changed to a point further along the direction of travel as the vehicle moves along the desired path. For the automated vehicle guidance and manual steering, the orientation of the vehicle should be accurately controlled with orientation error quickly reduced to a small value. The design requirements for angular orientation control are chosen to be zero steady state error, zero overshoot (for safety) and a settling time of 0.1 seconds. In addition, the performance requirements imply that the control system must be stable.

Control structure. To achieve the performance requirements, closed-loop feedback control may be used for the angular orientation control problem. Use of the error signal,

$$e(t) = Q_d(t) - Q(t), \quad (26)$$

will be required to create a controller that can reduce steady-state error to zero. The control effort, swashplate angle, can be adjusted according to the following equation:

$$\hat{\alpha}(t) = K_p e(t) + K_D \frac{d}{dt} Q(t). \quad (27)$$

Control design. The reasoning for choosing this controller structure can be seen by analyzing the closed loop dynamics by combining Eqs. (23), (26), and (27) to get,

$$\ddot{\Theta}(t) + (a + bK_D)\dot{\Theta}(t) + bK_p\Theta(t) = bK_p\Theta_d(t) \quad (28)$$

which is a second order differential equation. A steady state analysis, letting all time derivatives be zero in Eq. (28) and utilizing a steady value for Q_d , yields the following result,

$$Q(t) = Q_d \text{ as } t \rightarrow \infty. \quad (29)$$

This means that the steady-state error is zero. This is a consequence of the fact that the solution of the open loop system (without a feedback measurement) would increase linearly given a steady input effectively acting as an integrator as time increases. Systems with this characteristic

are known as type 1 systems and are able to track steady inputs with zero error in a feedback control system [2]. Notice that each coefficient on the left side of Eq. (28) has a control gain included. This will allow us to adjust the gains so that the characteristic equation of the differential equation can have any roots that we desire. It is the characteristic equation,

$$s^2 + (a + bK_D)s + bK_P = 0, \quad (30)$$

which has roots that can be used to find the solution of the differential equation. First the roots of the characteristic equation can be found as,

$$s_1, s_2 = \frac{a + bK_D}{2} \pm \frac{\sqrt{(a + bK_D)^2 - 4bK_P}}{2}. \quad (31)$$

The solution of the differential equation will contain exponential decay terms with the roots of the characteristic equation multiplied by time in the exponents. Since the system is second order, overshoot and oscillation in the response are possible if there are imaginary parts of the characteristic roots. One of the performance requirements is to have zero overshoot. Therefore, the control gains will be chosen so that the roots of the characteristic equation are real valued and negative to ensure zero overshoot (so that the solution is over-damped) and stability. To ensure that the characteristic equation will only have real roots, the following must be true,

$$(a + bK_D)^2 > 4bK_P. \quad (32)$$

The speed of response, in terms of the settling time, for a second order over-damped system can be described by the following approximation,

$$t_s \gg \frac{4}{S}, \quad (33)$$

where S is the real part of a root of the characteristic equation. If we select two identical real characteristic roots of value, S , then using Eq. (31) and substituting Eq. (33), the relationship between the settling time and the control gains can be derived as,

$$\frac{4}{t_s} = \frac{a + bK_D}{2} \Leftrightarrow K_D = \frac{\frac{8}{t_s} - a}{b}$$

and

$$(a + bK_D)^2 = 4bK_P \Leftrightarrow K_P = \frac{(a + bK_D)^2}{4b}. \quad (34)$$

Simple path following. On a plane, the cartesian location of the track-type tractor can be found using the fact that, neglecting slippage, the tractor can only move in the direction of the orientation angle, at given velocity,

$$x(t) = \int_0^t v(t) \cos Q(t) dt,$$

and

$$y(t) = \int_0^t v(t) \sin Q(t) dt. \quad (35)$$

Since the velocity may be changing at any instant in time, Eq. (35), should be integrated using numerical methods.

The following an example of a very simple method for achieving path guidance. In order to follow a path, a path must be generated and the desired orientation angle must be calculated and updated as the vehicle follows the path. Given any cartesian location of the track-type tractor, (x, y) , and a desired location, $(x_{d,i}, y_{d,i})$, the desired orientation angle can be computed using trigonometry,

$$Q_d = \tan^{-1} \left(\frac{y_{d,i} - y}{x_{d,i} - x} \right). \quad (36)$$

If an ordered set of $(x_{d,i}, y_{d,i})$ pairs, where $i = 1, 2, \dots, n$, representing a path is stored in a microcontroller based steering and guidance system, a simple method for choosing the next desired position (i.e., incrementing i by one) is,

$$\text{if, } (x_{d,i} - x)^2 + (y_{d,i} - y)^2 < r_d^2, \text{ then } i = i + 1, \quad (37)$$

where, r_d , is a desired minimum distance from the target location that is needed before switching to the next point on the path.

Results and Discussion

Orientation angle control. The control gains can be found by using the performance requirement for settling time, the values of the model parameters in the Table and the definition for a and b in Eq. (23) substituted into Eq. (34) to get $K_p = 101.7$ and $K_D = 2.64$. To check the results, a simulation has been created with a nominal velocity, $v_0 = 10$ kph. The input is a step change in the orientation angle of 1 degree. The differential equation in Eq. (28) is solved using the design results above and a unit step input for the desired orientation angle to get the results in Figs. 4-5. These results show that the response to the step change in the desired orientation angle is fast and there is zero steady-state error and zero overshoot. Also of interest is that the swashplate angle, $\hat{\alpha}$, is smaller than the maximum possible angle of one (recall that it is normalized) in Fig. 5.

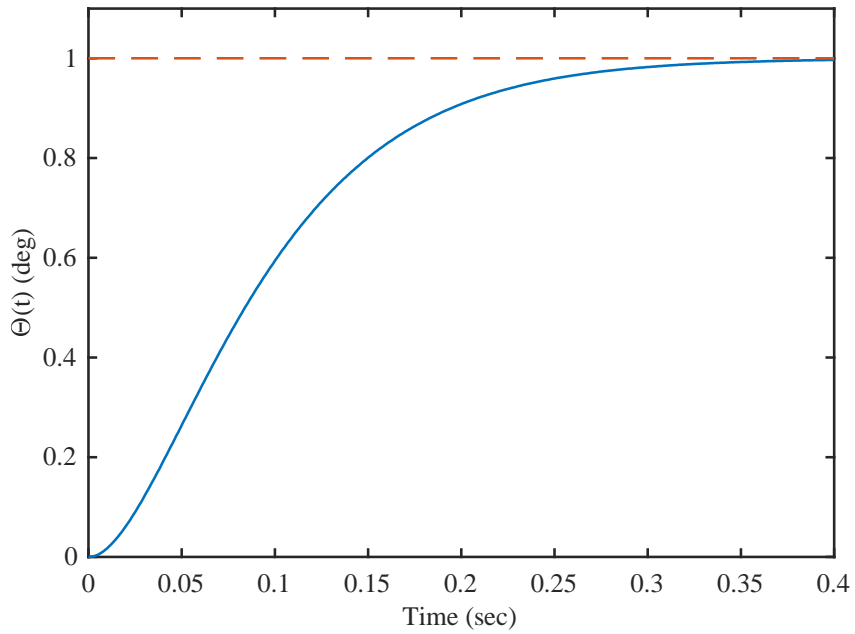


Figure 4. Response of the orientation angle (solid line) with automatic control given a step input for the desired orientation angle (dashed line)

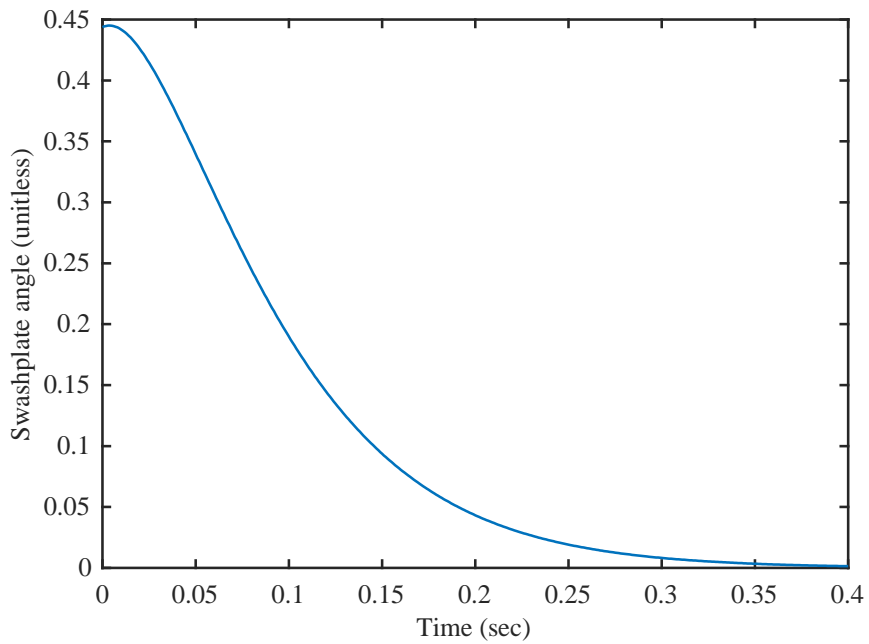


Figure 5. Swashplate angle response for the same simulation conditions as in Figure 4

Path tracking. A simulation was created to represent a position control application for the steering system (Figs. 6-10) using the simple path following equations (35)-(37) along with the dynamics of the control system Eq. (28) and the velocity dynamics, Eq. (21). A diagram of a MATLAB Simulink ® model used to implement all of the equations is given in Fig. 7. In the following simulation results, the nominal velocity has been chosen as $v_0 = 10$ kph and the minimum distance before switching to the next path location is $r_d = 5$ m. As can be seen from Fig. 7, the desired path (desired path coordinate pairs are plotted using stars) is a straight line with an offset displacement in the middle simulating avoidance of an obstacle. The simulated tractor position follows the path with a decreasing amount of error as the tractor approaches each desired coordinate location. To achieve this path, several adjustments to the desired orientation angle are made as the tractor approaches each successive target location and is directed by the path following system from one pair of target location coordinates to another (see Fig. 8). These adjustments to the path appear as step changes in the desired orientation angle, and it can be seen that on the timescale of the plot, the tractor follows these changes virtually instantaneously. The swashplate angle is always below one for these small steering adjustments (see Fig 9). With more path points to create a smoother path, these abrupt changes could be reduced to smaller adjustments and a smoother resulting path a travel for the tractor. In addition, more sophisticated path following algorithms, such as pure pursuit, where continuous paths are considered and curved trajectories onto the path are calculated, can be used to achieve smoother higher performance path following results [3].

Finally, the velocity response of the tractor is shown in Fig. 10. The velocity is an important factor in the computation of the location of the tractor and the response of the steering

system. The velocity is essentially constant over the entire simulation after a very short transient seen in Fig. 10.

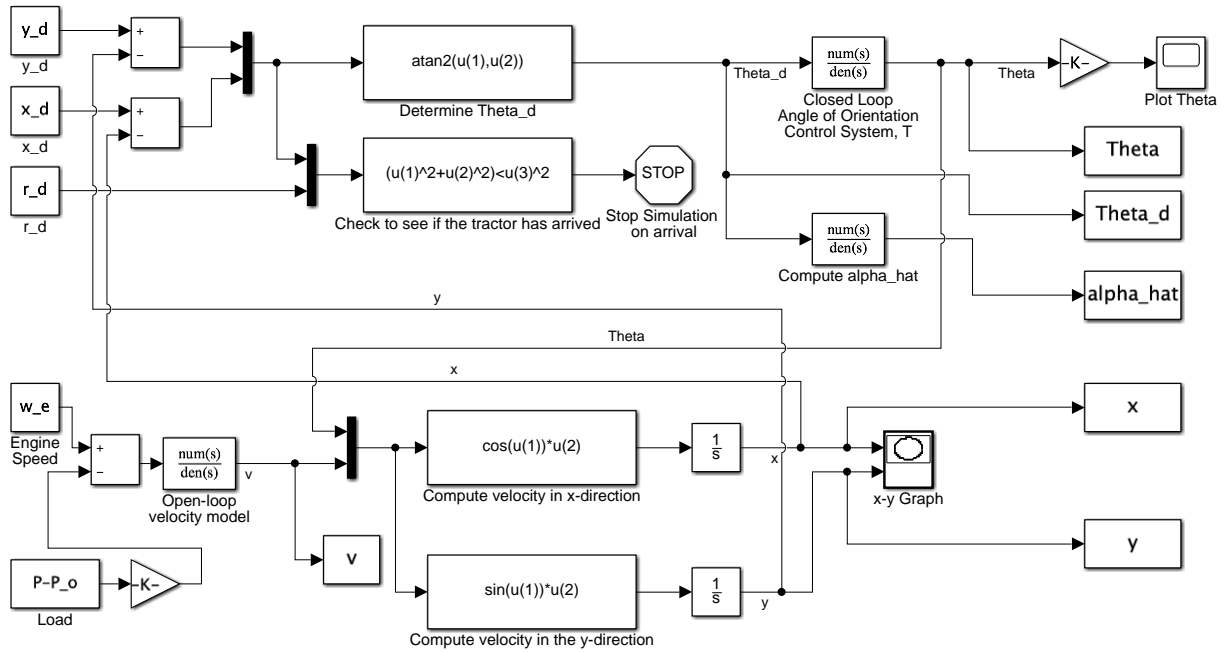


Figure 6. Diagram of the path tracking simulation

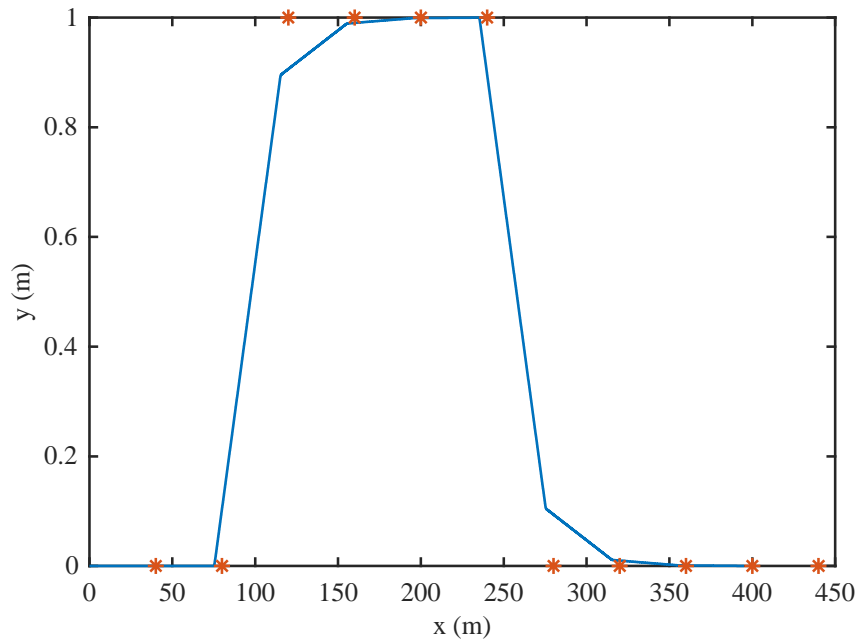


Figure 7. Path of the track-type tractor. Stars represent the desired path points.

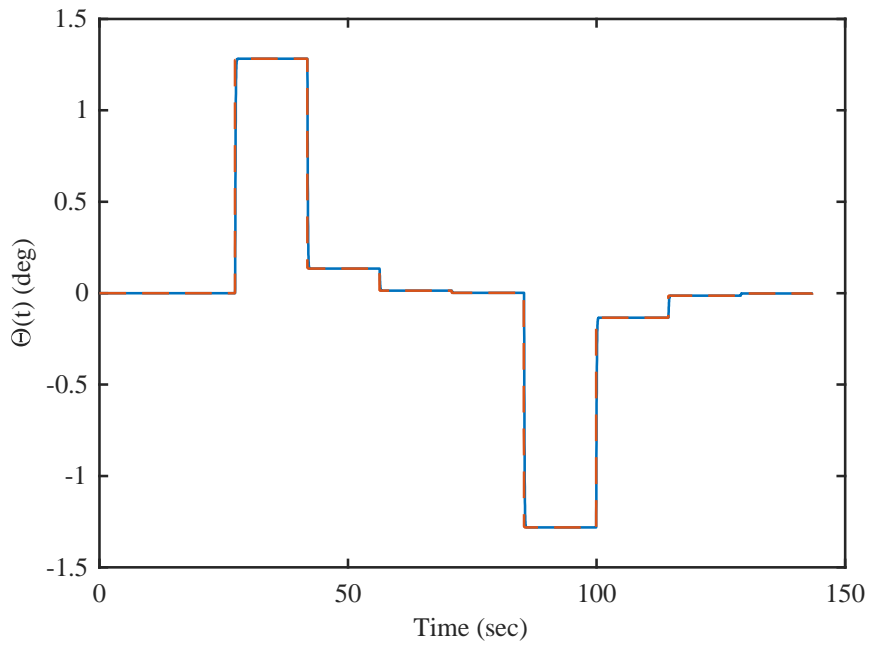


Figure 8. Actual orientation angle (solid line) and desired orientation angle (dashed line) for the path tracking simulation

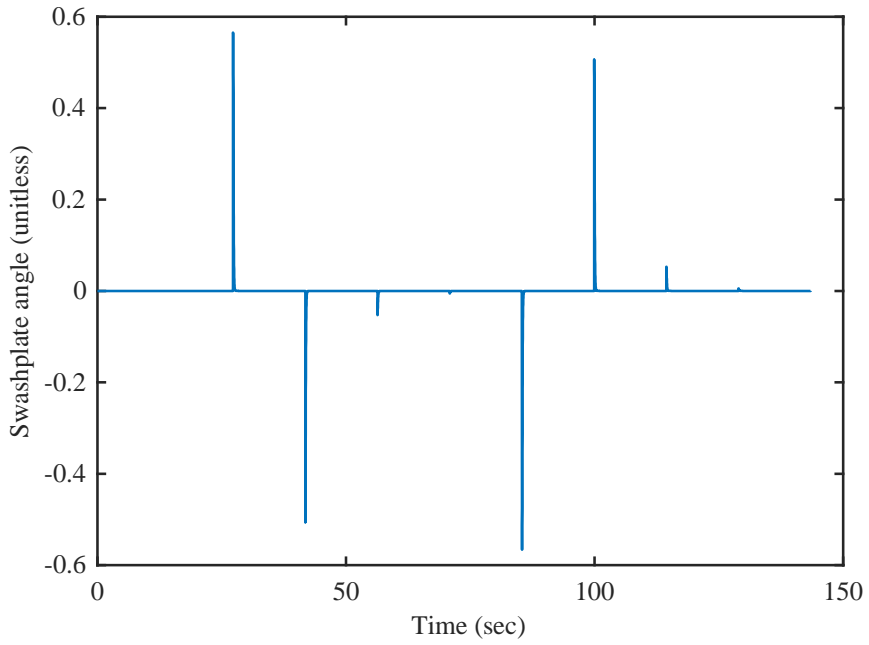


Figure 9. Swashplate angle for the path tracking simulation

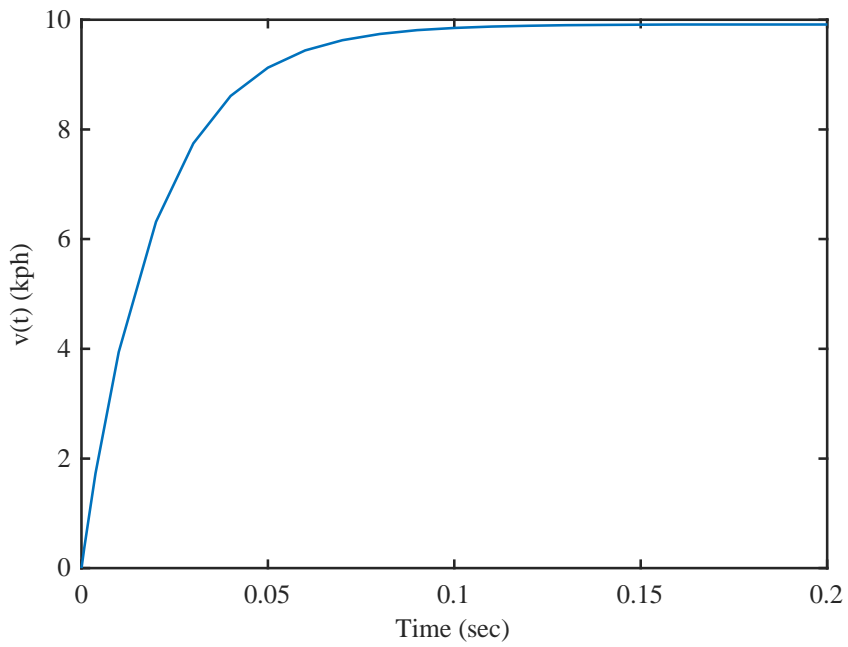


Figure 10. Velocity of the track-type tractor at the start of the path tracking simulation. The velocity remained constant during the remainder of the simulation.

Conclusion

A model of a track-type tractor was created that included the behavior of the vehicle driven by tracks which operate at a differential speed driven by a hydraulic steering pump and motor combination plus an average velocity driven by an engine. The dynamics of the orientation angle and the vehicle velocity are described by second order differential equations. An articulation angle control system was designed using proportional and derivative feedback terms to determine the swashplate angle of the steering pump. Simulations show that the control system is able to track step changes to the desired orientation angle and achieve zero steady state error and a fast response with zero overshoot in the orientation angle. This system was demonstrated using a simple path following algorithm as well. Simulations show that by making several step changes to the orientation angle, the tractor is able to follow a path that simulates an obstacle avoidance maneuver.

References

- [1] Peterson, J. T., N. D. Manring, and C. A. Kluever. 2004. Directional control of a dual-path hydrostatic transmission for a track-type vehicle. Proceedings of the 2004 ASME International Mechanical Engineering Congress and RD&D Expo. Anaheim, CA, USA, November 13-19.
- [2] Kluever, C.A., 2015. *Dynamic systems: modeling, simulation, and control*. John Wiley & Sons, Hoboken, NJ.

- [3] Coulter, R.C., 1992. *Implementation of the pure pursuit path tracking algorithm* (No. CMU-RI-TR-92-01). Carnegie-Mellon UNIV Pittsburgh PA Robotics INST.

ROBOT EXAMPLE

Descriptions

Figure 1 shows a schematic of a two degree-of-freedom robot, actuated by two linear, hydraulic actuators. The work objective for this robot is to lift a payload shown by the mass M and to place the load somewhere in the two-dimensional space shown by the vertical and horizontal axes. The motion of the robot is achieved by extending and / or retracting the hydraulic actuators. As shown in the figure, gravity g acts in the downward vertical-direction.

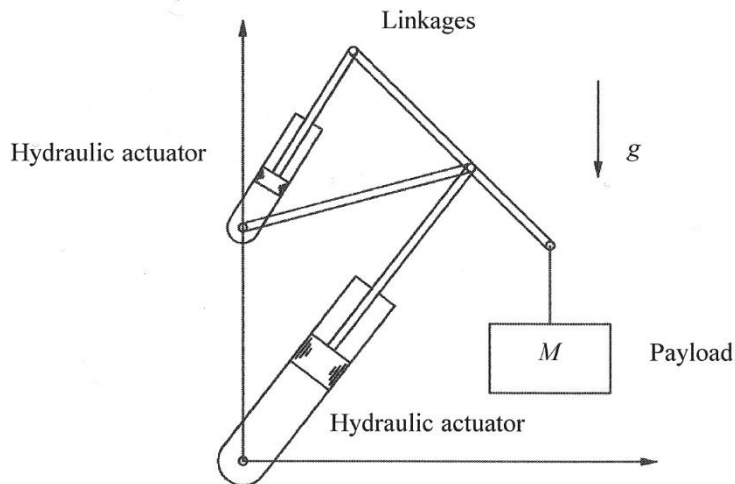
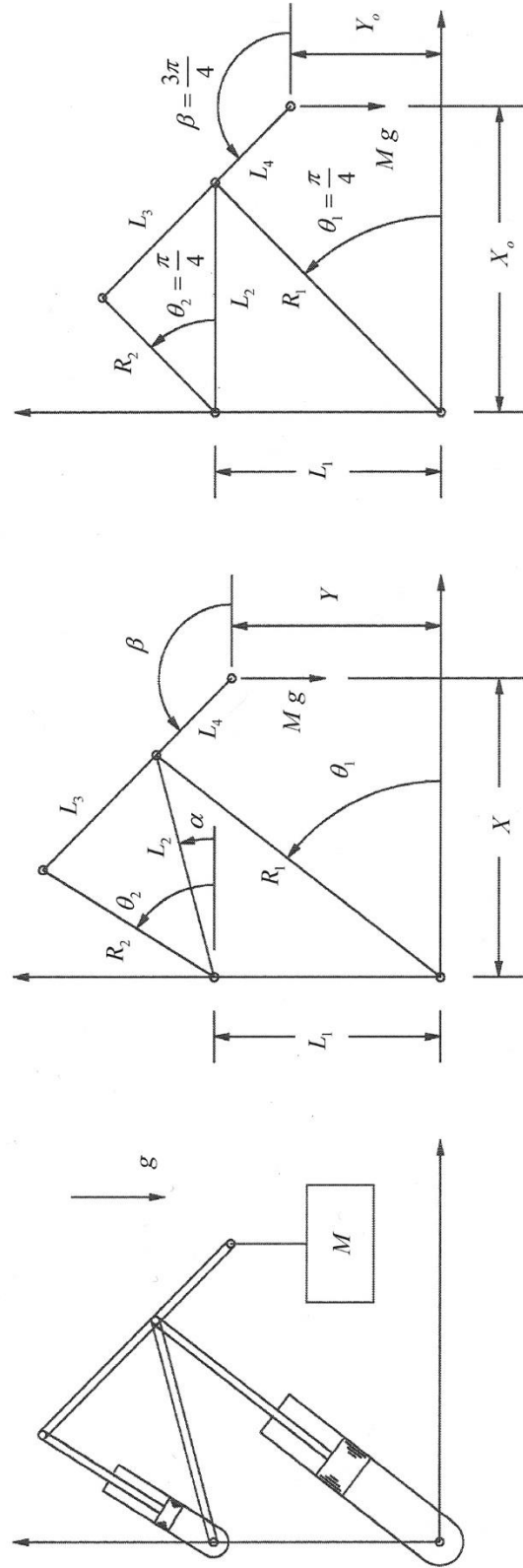


Figure 1. Schematic of the two degree-of-freedom robot

Figure 2 is presented to illustrate the geometry of the robot in both a general and nominal position. The actuators are shown to have variable lengths R_1 and R_2 , each actuator is oriented in space by the angles q_1 and q_2 respectively. The other fixed lengths shown in Fig. 1 are shown by the symbols $L_{1...4}$ with angular orientations given by $p/2$, a and b .



c) Nominal robot position, $\alpha = 0$

b) General robot position

a) Robot schematic

Figure 2. Robot positions

The objective of this robot is to locate the end effector at a location in space indicated by the vector $\boldsymbol{\rho} = X\hat{\mathbf{i}} + Y\hat{\mathbf{j}}$. This location is to be achieved while the robot lifts a gravitational load Mg shown in the downward direction. The paragraphs that follow will be used to analyze and model the actuation system shown Figs. 1 and 2.

Kinematic Analysis

Loop Closures. The robotic linkages in Fig. 1 contain three loop closures that may be described mathematically to study the overall kinematics of the system. For the first loop closure containing links R_1 , L_1 , and L_2 the following equations may be written to describe a mathematical relationship that must always be maintained if the loop is to remain closed:

$$\begin{aligned} 0 &= R_1 \cos(q_1) - L_2 \cos(a) \quad , \quad \text{and} \\ 0 &= R_1 \sin(q_1) - L_2 \sin(a) - L_1 \quad . \end{aligned} \tag{1}$$

Similarly, for the second loop closure containing links R_2 , L_2 , and L_3 the following equations may be written to mathematically describe the closure of this mechanical triad:

$$\begin{aligned} 0 &= R_2 \cos(q_2) - L_2 \cos(a) - L_3 \cos(b) \quad , \quad \text{and} \\ 0 &= R_2 \sin(q_2) - L_2 \sin(a) - L_3 \sin(b) \quad . \end{aligned} \tag{2}$$

Lastly, the bottom loop containing R_1 , L_4 , and the vector $\boldsymbol{\rho} = X\hat{\mathbf{i}} + Y\hat{\mathbf{j}}$ requires that the following mathematical relationships always be true:

$$\begin{aligned} 0 &= X - R_1 \cos(q_1) + L_4 \cos(b) \quad , \quad \text{and} \\ 0 &= Y - R_1 \sin(q_1) + L_4 \sin(b) \quad . \end{aligned} \tag{3}$$

Equations (1) through (3) contain six scalar equations with six unknowns: X , Y , q_1 , q_2 , a , and b . In this system of equations R_1 and R_2 are considered as controlled inputs to the linkage.

Due to the trigonometric functions in these equations, they do not have a closed-form solution and the unknowns must be determined using numerical methods.

Linearization. For the purposes of this study, we wish to illustrate the control of the robot by considering small motions about a nominal operating point for the end effector identified by the vector $\mathbf{p} = X_o \hat{\mathbf{i}} + Y_o \hat{\mathbf{j}}$. Near this operating point we will assume that

$q_1 = q_2 = \rho/4$, $a = 0$, $b = 3\rho/4$, and that the lengths of the hydraulic actuators are

$$R_1 = \frac{X_o + Y_o}{\sqrt{2}} + y_1 \quad , \quad R_2 = \frac{X_o + Y_o}{2\sqrt{2}} + y_2 \quad , \quad (4)$$

where y_1 and y_2 are the extended lengths of the actuators from their nominal positions. Setting y_1 and y_2 equal to zero, it may be shown that the fixed dimensions in Fig. 1 are given by

$$L_1 = L_2 = \frac{X_o + Y_o}{2} \quad , \quad L_3 = \frac{X_o + Y_o}{2\sqrt{2}} \quad \text{and} \quad L_4 = \frac{X_o - Y_o}{\sqrt{2}} \quad . \quad (5)$$

Using these fixed lengths and linearizing Eq.s (1) through (3) about the nominal operating point, the following solutions may be obtained for the unknown quantities:

$$\begin{aligned} X &= X_o + \sqrt{2} \frac{X_o - Y_o}{X_o + Y_o} (y_1 - y_2) \quad , \quad Y = Y_o + 2\sqrt{2} \frac{X_o}{X_o + Y_o} y_1 - \sqrt{2} \frac{X_o - Y_o}{X_o + Y_o} y_2 \quad , \\ q_1 &= \frac{\rho}{4} + \frac{\sqrt{2}}{X_o + Y_o} y_1 \quad , \quad q_2 = \frac{\rho}{4} + \frac{2\sqrt{2}}{X_o + Y_o} y_1 \quad , \\ a &= \frac{2\sqrt{2}}{X_o + Y_o} y_1 \quad , \quad \text{and} \quad b = \frac{3\rho}{4} + \frac{2\sqrt{2}}{X_o + Y_o} (y_1 - y_2) \quad . \end{aligned} \quad (6)$$

From this equation it can be seen that by altering the lengths of the hydraulic actuators y_1 and y_2 the location of the end effector is changed as are all the other variable angles. The reader should recall that these results are only valid near the operating point $\mathbf{p} = X_o \hat{\mathbf{i}} + Y_o \hat{\mathbf{j}}$. These results will be used in subsequent sections for modeling the robotic system.

Kinetic Analysis

Figure 3 shows a free body diagram of the link comprised of the fixed dimensions L_3 and L_4 . In this figure F_1 and F_2 are the forces from the two hydraulic actuators. The force P comes from link L_2 . For static equilibrium it may be shown that

$$\begin{aligned} 0 &= F_1 \cos(q_1) + F_2 \cos(q_2) + P \cos(a) \quad , \\ 0 &= F_1 \sin(q_1) + F_2 \sin(q_2) + P \sin(a) - M g \quad , \quad \text{and} \quad (7) \\ 0 &= -F_2 \sin(q_2) L_3 \cos(b) + F_2 \cos(q_2) L_3 \sin(b) - M g L_4 \cos(b) \quad . \end{aligned}$$

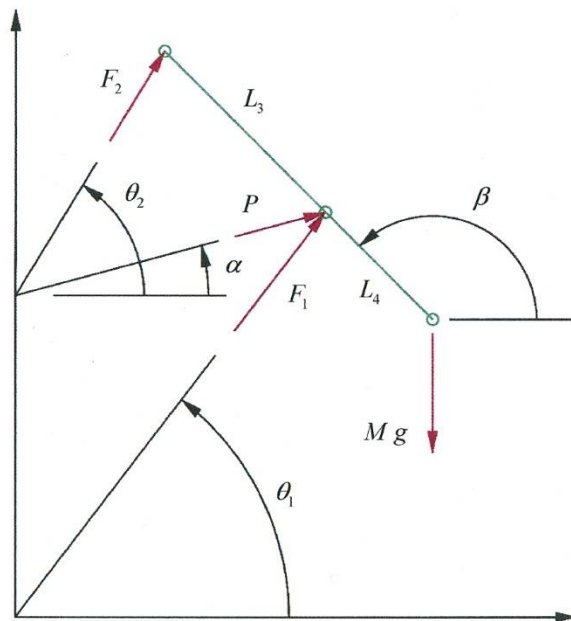


Figure 3. Free body diagram for link comprised of the fixed dimensions L_3 and L_4

By linearizing these equations for the nominal operating position of the linkage, and using Eq. (4) which depends upon the actuator extensions y_1 and y_2 , a simultaneous solution for these

equations produces the following result for the unknown forces F_1 , F_2 , and P :

$$\begin{aligned}
 F_1 &= \left(2\sqrt{2} \frac{X_o}{X_o + Y_o} + 4 \frac{2X_o - Y_o}{(X_o + Y_o)^2} y_1 - 4 \frac{X_o - Y_o}{(X_o + Y_o)^2} y_2 \right) M g \quad , \\
 F_2 &= - \left(\sqrt{2} \frac{X_o - Y_o}{X_o + Y_o} + 4 \frac{X_o - Y_o}{(X_o + Y_o)^2} (y_1 - y_2) \right) M g \quad , \\
 P &= - \left(1 + 2\sqrt{2} \frac{X_o - Y_o}{(X_o + Y_o)^2} y_1 \right) M g \quad .
 \end{aligned} \tag{8}$$

The actuator forces F_1 and F_2 will be used in the analysis which follows, to model the hydraulic system.

Hydraulic System Modeling

Actuator Description. The hydraulic actuators shown for the robot in Fig. 1 are controlled using a hydraulic power supply and a 4-way control valve for porting fluid in and out of the actuator. A detailed schematic for a single actuator is shown Fig. 4 where the controlled displacement of the actuator to the right is shown by the symbol y . The force acting on the actuator is shown by the symbol F and the fluid pressures on sides A and B of the actuator are given by the symbols P_A and P_B respectively. The pressurized areas on both sides of the actuator are given by A_A and A_B .

The 4-way valve shown in Fig. 4 moves back and forth in the x -direction in order to port fluid in and out of sides A and B of the actuator. The volumetric flow rate into side A is shown using the symbol Q_A while the volumetric flow rate out of side B is shown by the symbol Q_B .

These two flow rates result from the flow rates across the four metering lands of the valve which

are shown in Fig. 4 by the symbols Q_1 , Q_2 , Q_3 , and Q_4 . The valve is designed as an open-centered valve which means that the metering lands are open when the valve is in the null position $x = 0$. The nominal opening for each metering land is shown in Fig. 4 by the symbol u which is often called an underlapped dimension.

The hydraulic power supply to the open-centered 4-way valve is shown in Fig. 4 by a pressure compensated, variable displacement pump. This pump is automatically controlled to provide enough flow Q_p in order to maintain the supply pressure P_p . The torque and rotational speed of the pump shaft are shown by the symbols T and ω .

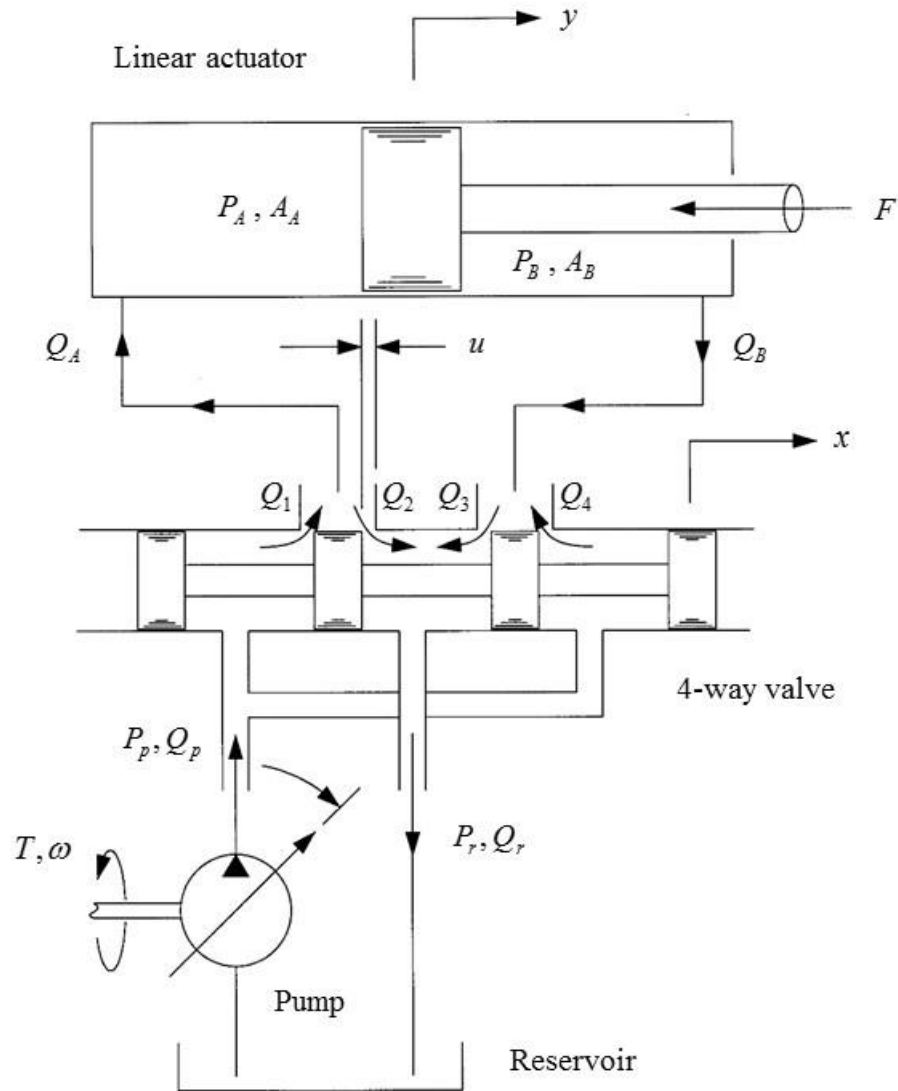


Figure 4. Schematic for a single hydraulic, linear actuator

The pump reservoir is shown to have a pressure P_r , which will be assumed to be atmospheric pressure in the analysis which follows. The volumetric flow rate returned to the reservoir by the 4-way valve is shown in Fig. 4 by the symbol Q_r .

Quasi-Steady Analysis. By neglecting the time rate-of-change of linear momentum for the actuator and its load, the following quasi-steady equation may be written to describe the load force acting on the actuator:

$$F = P_A A_A - P_B A_B \quad . \quad (9)$$

By neglecting the pressure transients on sides A and B of the actuator, the volumetric flow rate into the actuator on side A and out of the actuator on side B may be written as

$$Q_A = A_A \dot{y} \quad \text{and} \quad Q_B = A_B \dot{y} \quad (10)$$

where the dot notation over the symbol y is used to denote a time derivative. Equations (9) and (10) will provide the basic model for resisting and moving the actuator load.

Volumetric Flow Rates. As shown in Eq. (10) the volumetric flow rate in and out of the actuator is what moves the actuator to the right or left. For an incompressible fluid, the conservation of mass requires that

$$Q_A = Q_1 - Q_2 \quad \text{and} \quad Q_B = Q_3 - Q_4 \quad (11)$$

where each flow rate is shown schematically in Fig. 4. If we assume that each port area for each metering land on the 4-way valve opens linearly with respect to the valve displacement x , then using the classical orifice equation the volumetric flow rate across each metering land may be written as

$$\begin{aligned} Q_1 &= h(u+x)C_d\sqrt{\frac{2}{\rho}(P_p - P_A)} \quad , \quad Q_2 = h(u-x)C_d\sqrt{\frac{2}{\rho}(P_A - P_r)} \quad , \\ Q_3 &= h(u+x)C_d\sqrt{\frac{2}{\rho}(P_B - P_r)} \quad , \quad Q_4 = h(u-x)C_d\sqrt{\frac{2}{\rho}(P_p - P_B)} \quad . \end{aligned} \quad (12)$$

In this result h is the area gradient of the valve port, u is the underlapped dimension as previously noted, C_d is the dimensionless discharge coefficient, ρ is the fluid density, and all other variables have been previously defined. Substituting Eq. (12) into Eq. (11) and linearizing the result about nominal operating conditions produces the following linearized results for the volumetric flow rate in and out of the actuator:

$$\begin{aligned}
Q_A &= K_{q_A} (x - x_o) - K_{c_A} (P_A - P_{A_o}) \\
Q_B &= K_{q_B} (x - x_o) + K_{c_B} (P_B - P_{B_o}) \quad ,
\end{aligned} \tag{13}$$

where the subscript “o” denotes a nominal condition and the flow gains and pressure-flow coefficients are given by

$$\begin{aligned}
K_{q_A} &= h C_d \sqrt{\frac{2}{r} P_p} \left(\sqrt{1 - \frac{P_{A_o}}{P_p}} + \sqrt{\frac{P_{A_o}}{P_p}} \right) \quad , \quad K_{c_A} = \frac{u h C_d}{\sqrt{2 r P_p}} \left(\frac{1 + \frac{x_o}{u}}{\sqrt{1 - \frac{P_{A_o}}{P_p}}} + \frac{1 - \frac{x_o}{u}}{\sqrt{\frac{P_{A_o}}{P_p}}} \right) \quad , \\
K_{q_B} &= h C_d \sqrt{\frac{2}{r} P_p} \left(\sqrt{1 - \frac{P_{B_o}}{P_p}} + \sqrt{\frac{P_{B_o}}{P_p}} \right) \quad , \quad K_{c_B} = \frac{u h C_d}{\sqrt{2 r P_p}} \left(\frac{1 + \frac{x_o}{u}}{\sqrt{1 - \frac{P_{B_o}}{P_p}}} + \frac{1 - \frac{x_o}{u}}{\sqrt{\frac{P_{B_o}}{P_p}}} \right) \quad .
\end{aligned} \tag{14}$$

Nominal Operating Condition. In order to evaluate the nominal operating conditions of the system we recognize at steady-state conditions (no motion) $Q_A = Q_B = 0$, which means that $Q_1 - Q_2 = 0$ and $Q_3 - Q_4 = 0$. Using these relationships with Eq. (12) it may be shown that the following nominal-relationship must exist at steady-state conditions:

$$\left(\frac{u + x_o}{u - x_o} \right)^2 = \frac{P_{A_o}}{P_p - P_{A_o}} = \frac{P_p - P_{B_o}}{P_{B_o}} \quad . \tag{15}$$

From this result it may be shown that the following relationship must exist for the steady-state pressures in the actuator:

$$P_p = P_{A_o} + P_{B_o} \quad . \tag{16}$$

Using this result with Eq. (9) produces the following equations for the nominal pressures on both sides of the actuator:

$$P_{A_o} = \frac{A_B P_p + F_o}{A_A + A_B} \quad \text{and} \quad P_{B_o} = \frac{A_A P_p - F_o}{A_A + A_B} \quad (17)$$

where F_o is the nominal force acting on the actuator. Using either one of these results with Eq.

(15) the following expression may be written

$$\left(\frac{u + x_o}{u - x_o} \right)^2 = \frac{A_B P_p + F_o}{A_A P_p - F_o} \quad (18)$$

Solving for x_o from this equation produces the following result:

$$x_o = \frac{C - 1}{C + 1} u \quad \text{where} \quad C = \sqrt{\frac{A_B P_p + F_o}{A_A P_p - F_o}} \quad (19)$$

These results may be used to model the hydraulic actuator as a linear system near the nominal operating points.

Summary. Using the preceding analysis with Eqs. (9) and (10), the actuator velocity and the fluid pressure on side A and B may be solved for algebraically as

$$\dot{y} = \left(\frac{A_A K_{c_B} K_{q_A} + A_B K_{c_A} K_{q_B}}{A_B^2 K_{c_A} + A_A^2 K_{c_B}} \right) (x - x_o) - \left(\frac{K_{c_A} K_{c_B}}{A_B^2 K_{c_A} + A_A^2 K_{c_B}} \right) (F - F_o) \quad (20)$$

and

$$P_A = P_{A_o} + \left(\frac{A_B (A_B K_{q_A} + A_A K_{q_B})}{A_B^2 K_{c_A} + A_A^2 K_{c_B}} \right) (x - x_o) + \left(\frac{A_A K_{c_B}}{A_B^2 K_{c_A} + A_A^2 K_{c_B}} \right) (F - F_o) \quad (21)$$

$$P_B = P_{B_o} - \left(\frac{A_A (A_A K_{q_B} - A_B K_{q_A})}{A_B^2 K_{c_A} + A_A^2 K_{c_B}} \right) (x - x_o) - \left(\frac{A_B K_{c_A}}{A_B^2 K_{c_A} + A_A^2 K_{c_B}} \right) (F - F_o)$$

Equation (20) is particularly useful for modeling the motion of each linear actuator in the robotic system. For each actuator, the disturbance force F may be applied using results from Eq.(8).

Parameter Design

The design of the system will proceed using the following assumptions. The mass of the load is $M = 1000$ kg. The nominal position of the load is assumed to be, $X_o = 2$ m, and $Y_o = 1$ m. The nominally loaded operating velocity of the hydraulic cylinders is $v_o = 0.25$ m/sec and the hydraulic pump pressure is assumed to be constant at $P_p = 10$ MPa. . The discharge coefficient of the valves is assumed to be $C_d = 0.62$, which is consistent with a sharp-edged orifice. The density of the hydraulic fluid is $\gamma = 0$ The full stroke capability of the hydraulic cylinders are each $y = \pm 0.25$ m. To determine the remaining design parameters of the robot hydraulic system, a number of design conditions will be considered and flow losses, leakage, and friction will be neglected. Subscripts 1 and 2 are used to denote parameters and quantities that are specific to either cylinder/valve 1 or cylinder/valve 2.

Actuators. The hydraulic cylinders serve as actuators for the system. The areas of the cylinder piston (A and B sides for cylinder 1 and 2) need to be determined for the load under two design conditions. The load on the cylinders can be calculated using the forces in Eq. (8) for each cylinder. For cylinder 1, the first design condition considered is a nominal load (force when $y = 0$ for both cylinders), $P_{A_1} = P_{A_{1,o}} = (2/3)P_p$, and $P_{B_1} = P_{B_{1,o}} = (1/3)P_p$ and $y_1 = y_2 = 0$. Using the design conditions and Eqs. (8) and (9) it can be shown that,

$$\frac{2}{3}A_{A_1} + \frac{1}{3}A_{B_1} = \frac{F_{1,o}}{P_p},$$

where

$$F_{1,o} = 2\sqrt{2}Mg \frac{X_o}{X_o + Y_o}.$$

(22)

For cylinder 1, the second design condition considered is a working load (force when $y = y_{max}$, a displacement associated with a maximum force on both cylinders according to Eq. (8)),

$P_{A_1} = \frac{7}{8} P_p$, and $P_{B_1} = \frac{1}{4} P_p$. Using these design conditions, it can be shown that,

$$\frac{7}{8} A_{A_1} + \frac{1}{8} A_{B_1} = \frac{F_{1,o} + F_{1,w}}{P_p},$$

(23)

where

$$F_{1,w} = F_1(y_{1,max}, y_{2,max}) - F_{1,o}.$$

Solving these two equations simultaneously, allows for the computation of the cylinder areas for cylinder 1,

$$A_{A_1} = \frac{8 F_{1,o} + F_{1,w}}{5 P_p} - \frac{3 F_{1,o}}{5 P_p}$$

$$A_{B_1} = \frac{16 F_{1,o} + F_{1,w}}{5 P_p} - \frac{21 F_{1,o}}{5 P_p}$$

(24)

Using a similar procedure and noting that cylinder 2 has loads such that the cylinder forces are negative, the cylinder areas for cylinder 2 can be found as,

$$A_{A_2} = -8 \frac{F_{2,o} + F_{2,w}}{P_p} + 9 \frac{F_{2,o}}{P_p}$$

$$A_{B_2} = -2 \frac{F_{2,o} + F_{2,w}}{P_p} + \frac{F_{2,o}}{P_p}$$

(25)

Using these equations, the cylinder areas are found to be,

$$A_{A_1} = 35.9, A_{B_1} = 16.38, A_{A_2} = 12.82, \text{ and } A_{B_2} = 8.98 \text{ cm}^2.$$

Valves. The hydraulic valve parameters can be designed to fit design conditions with nominal pressures due to nominal loading and a given velocity and neglecting any flow losses. For valve 1, the design condition is for a nominal load velocity, v_o , at a displacement such that ,

$x_1 - x_{1,o} = 1/4(u_1 - x_{1,o})$, with nominal pressures on the both the A and B ports of the valve

($P_{A_1} = P_{A_{1,o}}$ and $P_{B_1} = P_{B_{1,o}}$). Under these conditions, and noting that $Q_{A_1} = v_o A_{A_1}$, Eq (13) can be

used to find the following:

$$K_{q_{A1}} = \frac{4v_o A_{A_1}}{u_1 - x_{1,o}} \quad (26)$$

By letting $4u_1 = h$ and substituting Eq. (26) into Eq. (14), an expression for the valve underlap dimension can be found as,

$$u_1 = \sqrt{\frac{v_o A_{A_1}}{S_{A_1} (1 - \hat{x}_{1,o})}},$$

where

$$\hat{x}_{1,o} = \frac{x_{1,o}}{u_1} = \frac{C_1 - 1}{C_1 + 1} \quad (27)$$

and

$$S_{A_1} = C_d \sqrt{P_p} \frac{2}{r} \left(\sqrt{1 - \frac{P_{A_{1,o}}}{P_p}} + \sqrt{\frac{P_{A_{1,o}}}{P_p}} \right).$$

A similar procedure can be used to find the underlap dimension for valve 2,

$$u_2 = \sqrt{\frac{v_o A_{B_2}}{S_{A_2} (1 - \hat{x}_{2,o})}},$$

where

$$\hat{x}_{2,o} = \frac{x_{2,o}}{u_2} = \frac{C_2 - 1}{C_2 + 1} \quad (28)$$

and

$$S_{B_2} = C_d \sqrt{P_p} \frac{2}{r} \left(\sqrt{1 - \frac{P_{B_{2,o}}}{P_p}} + \sqrt{\frac{P_{B_{2,o}}}{P_p}} \right).$$

Using these equations the overlapped dimensions are found to be, $u_1 = 2.6$ mm, and $u_2 = 1.2$ mm. With the cylinder areas and overlapped dimensions computed all of the linearized valve coefficients can be computed using Eq. (14).

Position Control

Control design requirements. Typical goals for controlling a robotic positioning system are to be able to position the load accurately and move between positions quickly. In addition, overshoot of the desired position is generally to be avoided to prevent safety hazards and damage to the surroundings. Therefore, the performance requirements are as follows:

1. Zero steady state positioning error
2. Zero overshoot
3. Fast settling time, $t_s < 1$ sec.

System characteristics. The characteristics of the system dynamics can be used to motivate decisions about what type of control structure should be used for position control. The control system design will rely on the linearized system equations and the deviations from the nominal conditions will be considered for control using the following definitions,

$$\begin{aligned}
 dy_1 &= y_1 - y_{1,o}, \\
 dy_2 &= y_2 - y_{2,o}, \\
 dF_1 &= F_1 - F_{1,o}, \\
 dF_2 &= F_2 - F_{2,o}, \\
 dx_1 &= x_1 - x_{1,o}, \\
 &\text{and} \\
 dx_2 &= x_2 - x_{2,o}.
 \end{aligned} \tag{29}$$

The system to be controlled can be found by combining Eqs. (8) and (20) for each cylinder,

$$\dot{y}_1 = -MgB_1A_1 dy_1 + MgB_2A_1 dy_2 + b_1 dx_1$$

and

$$\dot{y}_2 = MgB_2A_2 dy_1 - MgB_2A_2 dy_2 + b_2 dx_2,$$

where

$$A_1 = \frac{K_{c_{A1}} K_{c_{B1}}}{A_{B_1}^2 K_{c_{A1}} + A_{A_1}^2 K_{c_{B1}}}, \quad (30)$$

$$A_2 = \frac{K_{c_{A2}} K_{c_{B2}}}{A_{B_2}^2 K_{c_{A2}} + A_{A_2}^2 K_{c_{B2}}},$$

$$B_1 = 4 \frac{2X_o - Y_o}{X_o + Y_o}, \text{ and}$$

$$B_2 = 4 \frac{X_o - Y_o}{(X_o + Y_o)^2}.$$

The output position of the system to be controlled can be calculated as,

$$X = \sqrt{2} \frac{X_o - Y_o}{X_o + Y_o} dy_1 - \sqrt{2} \frac{X_o - Y_o}{X_o + Y_o} dy_2$$

and

$$Y = 2\sqrt{2} \frac{X_o}{X_o + Y_o} dy_1 - \sqrt{2} \frac{X_o - Y_o}{X_o + Y_o} dy_2. \quad (31)$$

These equations can be written in linear state space form as,

$$\dot{\mathbf{z}} = \mathbf{Az} + \mathbf{Bu},$$

and

$$\mathbf{y} = \mathbf{Cz}. \quad (32)$$

In this form the matrices and vectors for the state derivative, state and output are defined as follows,

$$\begin{aligned}
\mathbf{A} &= \begin{bmatrix} -MgB_1A_1 & MgC_1A_1 \\ MgB_2A_2 & -MgB_2A_2 \end{bmatrix}, \quad \mathbf{B} = \begin{bmatrix} b_1 & 0 \\ 0 & b_2 \end{bmatrix}, \\
\mathbf{C} &= \begin{bmatrix} \sqrt{2} \frac{X_o - Y_o}{X_o + Y_o} & -\sqrt{2} \frac{X_o - Y_o}{X_o + Y_o} \\ 2\sqrt{2} \frac{X_o}{X_o + Y_o} & -\sqrt{2} \frac{X_o - Y_o}{X_o + Y_o} \end{bmatrix}, \\
\dot{\mathbf{z}} &= \begin{bmatrix} \dot{y}_1 \\ \dot{y}_2 \end{bmatrix}, \quad \mathbf{z} = \begin{bmatrix} \delta y_1 \\ \delta y_2 \end{bmatrix}, \quad \mathbf{u} = \begin{bmatrix} \delta x_1 \\ \delta x_2 \end{bmatrix}, \quad \text{and } \mathbf{y} = \begin{bmatrix} \delta X \\ \delta Y \end{bmatrix}.
\end{aligned} \tag{33}$$

The state space form is a standard way of expressing dynamic systems and many methods exist for controlling systems of this form. Using the equations in this section and the Parameter Design section, state space matrices can be calculated as,

$$\begin{aligned}
\mathbf{A} &= \begin{bmatrix} -0.9424 & 0.1047 \\ 0.1744 & -0.1744 \end{bmatrix}, \quad \mathbf{B} = \begin{bmatrix} 459.0741 & 0 \\ 0 & 103.7509 \end{bmatrix}, \\
\text{and } \mathbf{C} &= \begin{bmatrix} 0.4714 & -0.4714 \\ 1.8856 & -0.4714 \end{bmatrix}.
\end{aligned} \tag{34}$$

The stability of the system can be determined by computing the eigenvalues of the \mathbf{A} matrix which are the same as the roots of the characteristic equation, $s_1 = -0.9655$ and $s_2 = -0.1513$. These eigenvalues indicate that the system is stable and that there will be no integrator action (no eigenvalue at the origin). The control system structure will need to add integration which will ensure zero steady-state error when there is a step change in the desired position. A convenient transformation can be made to a new set of states which are the same as the outputs. This transformation can be made by applying the following substitution to Eq. (32) so that,

$$\mathbf{z} = \mathbf{C}^{-1}\mathbf{y} \Rightarrow \begin{cases} \dot{\mathbf{y}} = \mathbf{A}_y\mathbf{y} + \mathbf{B}_y\mathbf{u} \\ \mathbf{y} = \mathbf{C}_y\mathbf{y} \end{cases}, \text{ and} \quad (35)$$

$$\mathbf{A}_y = \mathbf{C}\mathbf{A}\mathbf{C}^{-1}, \mathbf{B}_y = \mathbf{C}\mathbf{B}, \text{ and } \mathbf{C}_y = \mathbf{I}.$$

Control structure. Position control requires a desired reference position vector,

$$\mathbf{r} = \begin{bmatrix} X_d & Y_d \end{bmatrix}^T, \text{ which can be compared to the position determined from measured feedback}$$

signals. The control structure could use feedback of the all states in Eq. (35) but would still lack the integrator effect needed for the control system to achieve zero steady-state error. To obtain the integrator action, the states will be augmented to with an additional integrator state vector, \mathbf{w} , which is the time integral of $\mathbf{y} - \mathbf{r}$. An illustrative example showing the addition of integrator states can be found in [1]. To apply this method to the robot dynamics, the state space system in Eq. (35) can be modified by augmenting it with negative error integral states and a reference input as follows,

$$\begin{bmatrix} \dot{\mathbf{y}} \\ \dot{\mathbf{w}} \end{bmatrix} = \begin{bmatrix} \mathbf{A}_y & \mathbf{0}_{2 \times 2} \\ \mathbf{I}_{2 \times 2} & \mathbf{0}_{2 \times 2} \end{bmatrix} \begin{bmatrix} \mathbf{y} \\ \mathbf{w} \end{bmatrix} + \begin{bmatrix} \mathbf{B}_y \\ \mathbf{0}_{2 \times 2} \end{bmatrix} \mathbf{u} + \begin{bmatrix} \mathbf{0}_{2 \times 2} \\ -\mathbf{I}_{2 \times 2} \end{bmatrix} \mathbf{r} \quad (36)$$

$$\text{and } \mathbf{y} = \begin{bmatrix} \mathbf{C}_y & \mathbf{0}_{2 \times 2} \end{bmatrix} \begin{bmatrix} \mathbf{y} \\ \mathbf{w} \end{bmatrix}.$$

This equation can be made simpler by including a few definitions as follows:

$$\mathbf{z}_a = \begin{bmatrix} \mathbf{y} \\ \mathbf{w} \end{bmatrix}, \dot{\mathbf{z}}_a = \begin{bmatrix} \dot{\mathbf{y}} \\ \dot{\mathbf{w}} \end{bmatrix}, \mathbf{A}_a = \begin{bmatrix} \mathbf{A}_y & \mathbf{0}_{2 \times 2} \\ \mathbf{I}_{2 \times 2} & \mathbf{0}_{2 \times 2} \end{bmatrix}, \mathbf{B}_a = \begin{bmatrix} \mathbf{B}_y \\ \mathbf{0}_{2 \times 2} \end{bmatrix}, \mathbf{B}_r = \begin{bmatrix} \mathbf{0}_{2 \times 2} \\ -\mathbf{I}_{2 \times 2} \end{bmatrix}, \mathbf{C}_a = \begin{bmatrix} \mathbf{C}_y & \mathbf{0}_{2 \times 2} \end{bmatrix}$$

$$\Rightarrow \dot{\mathbf{z}}_a = \mathbf{A}_a \mathbf{z}_a + \mathbf{B}_a \mathbf{u} + \mathbf{B}_r \mathbf{r} \text{ and } \mathbf{y} = \mathbf{C}_a \mathbf{z}_a. \quad (37)$$

A full state feedback control system can be applied to the system by,

$$\mathbf{u} = -\mathbf{K} \mathbf{z}_a. \quad (38)$$

The closed-loop control system dynamics can be found by substituting the above equation into Eq. (37) to get,

$$\dot{\mathbf{z}}_a = (\mathbf{A}_a - \mathbf{B}_a \mathbf{K}) \mathbf{z}_a + \mathbf{B}_r \mathbf{r} \text{ and } \mathbf{y} = \mathbf{C}_a \mathbf{z}_a. \quad (39)$$

Control design. The full state feedback control gain, \mathbf{K} , can now be designed for the augmented system by means of pole placement. Pole placement refers to specifying the location of the eigenvalues (poles) of the closed loop characteristic equation. The desired pole locations can be selected to have negative real parts to ensure stability, have no imaginary parts to avoid overshoot, and have a magnitude greater than 4 times the inverse of the desired settling time to achieve the desired speed of response. Therefore, the poles of our fourth-order augmented system with full state feedback are selected to be, $s_{1,2,3,4} = -4, -4, -6, -8$. To find the control gain, \mathbf{K} , is chosen so that Eq. (39) has the desired closed-loop pole locations, i.e.

$$\mathbf{K} \text{ so that } s_{1,2,3,4} = -4, -4, -6, -8 \text{ satisfies the equation } \det[s\mathbf{I} - (\mathbf{A}_a - \mathbf{B}_a \mathbf{K})] = 0. \quad (40)$$

To find pole placement gains, a variety of mathematical tools may be used which are often based on Akerman's formula (for details, see ref [2-3]). The required matrices can be found by using the equations in this section and numerical parameters from previous sections so that the solution for \mathbf{K} can be found numerically.

Results and Discussion

Controller design. The control design that is a solution for Eq. (40), found using MATLAB's `place()` command, is

$$\mathbf{K} = \begin{bmatrix} -0.0177 & 0.0141 & -0.0493 & 0.0370 \\ -0.3236 & 0.0682 & -0.8724 & 0.1636 \end{bmatrix}. \quad (41)$$

This controller may be used in Eq. (39). The resulting closed-loop differential equations can be numerically integrated to simulate the robot position control system so that the simulated performance can be compared to the design requirements.

Simulation results. The following figures show the simulation results for the closed-loop system with a step change in the reference input of magnitude, $\mathbf{r} = \begin{bmatrix} 0.05 & 0.20 \end{bmatrix}^T$ m.

The simulated response of the two cartesian coordinates of the end effector is shown in Fig. 5. From this figure, it can be seen that the steady state error is zero due to the integral action of the augmented plant and the time response has zero overshoot and the settling time is just over one second due to the selection of the pole locations. The valve displacement is plotted for the simulation in Fig. 6. The valve displacement is small compared to the underlap dimension for both valves. Figure 7 shows the trajectory of the end effector during the simulation. The end effector takes nearly a straight path from the nominal position to the final position.

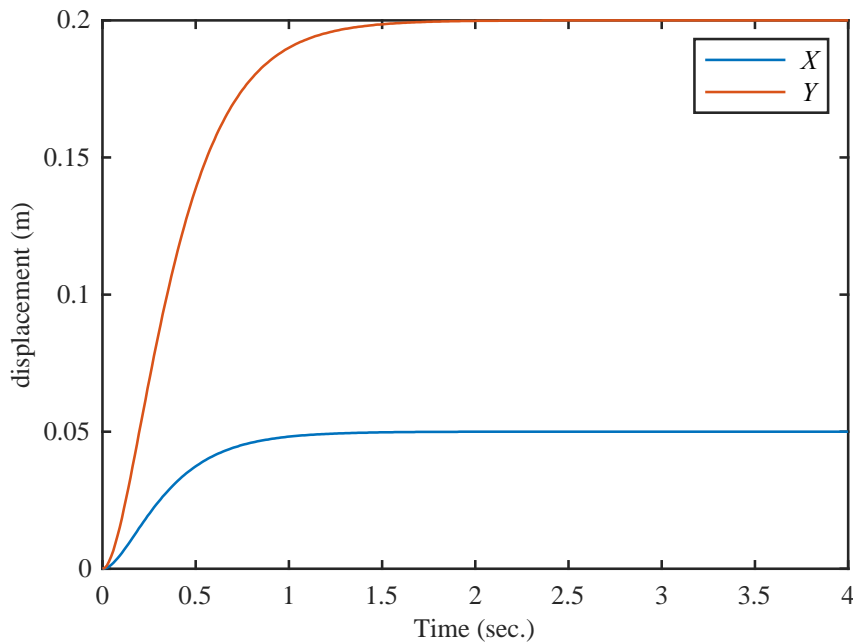


Figure 5. Reference step response of the displacement of the X and Y from the nominal position

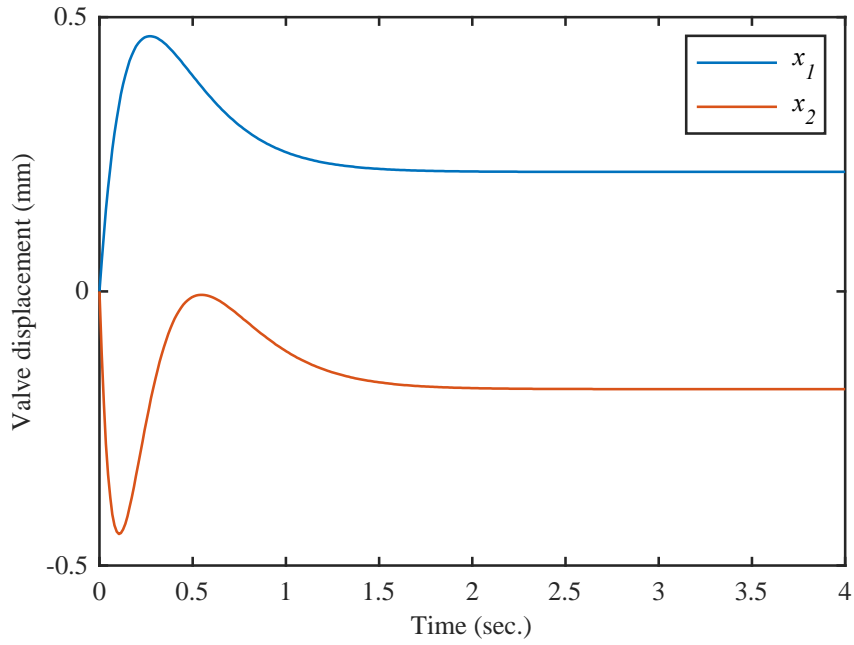


Figure 6. Reference step response of the displacement of the valves from the nominal positions

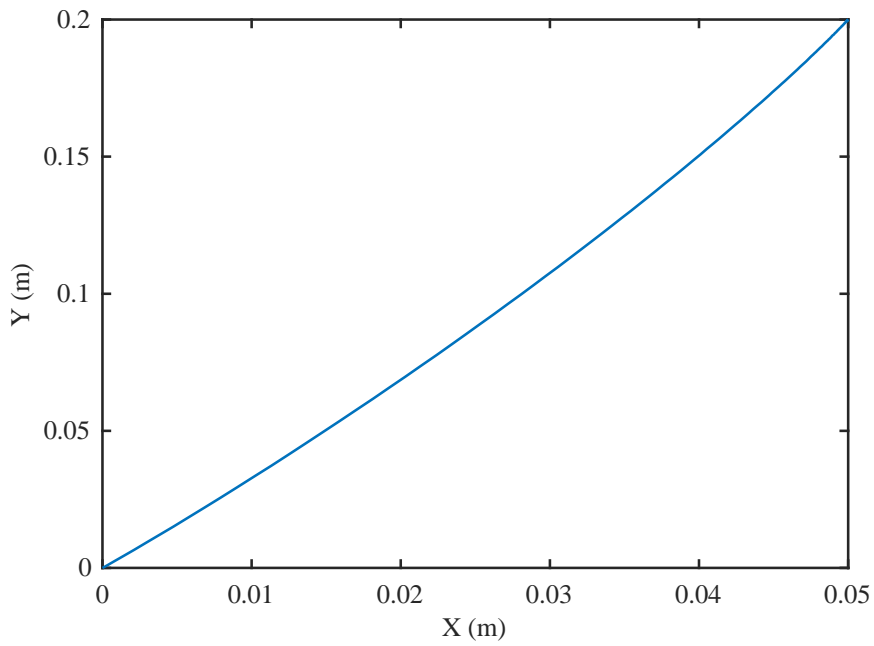


Figure 7. Plot of the trajectory of the end effector starting at the nominal position

Conclusion

In this case study, a hydraulic system connected to a two-degree-of-freedom robot linkage is presented. A model of the robot which utilizes a linkage connected to two valve-controlled hydraulic cylinders for actuation is derived and linearized about an operating point. The design of the robot hydraulic system parameters is shown to be a straightforward process that includes solving for critical parameters by considering several operating conditions. The control design employs error integrators which are augmented to the dynamic system model prior to designing control gains using a common pole placement method. The response of the system with the controller is acceptable in terms of the stated performance requirements which include zero steady-state error, zero overshoot, and a settling time of 1 second. The methods presented here can be applied to a variety of hydraulically operated machines with similar characteristics such as cranes, excavators and others which use valve-controlled hydraulic cylinders to actuate linkages.

References

- [1] <http://ctms.engin.umich.edu/CTMS/index.php?example=MotorPosition§ion=ControlStateSpace>
- [2] Dorf, R., and R. Bishop. 1995. *Modern Control Systems*, 7th ed. Addison-Wesley, Reading, MA
- [3] <https://www.mathworks.com/help/control/ref/place.html#bq1no8b-1>